NASA Technical Memorandum 72857

CORRELATION OF PREDICTED AND MEASURED THERMAL STRESSES ON A TRUSS-TYPE AIRCRAFT STRUCTURE

Jerald M. Jenkins, Lawrence S. Schuster, and Alan L. Carter

November 1978

NASA

NASA Technical Memorandum 72857

CORRELATION OF PREDICTED AND MEASURED THERMAL STRESSES ON A TRUSS-TYPE AIRCRAFT STRUCTURE

Jerald M. Jenkins, Lawrence S. Schuster, and Alan L. Carter

Dryden Flight Research Center
Edwards, California

National Aeronautics and
Space Administration

1978

CORRELATION OF PREDICTED AND MEASURED THERMAL STRESSES ON A TRUSS-TYPE AIRCRAFT STRUCTURE

Jerald M. Jenkins, Lawrence S. Schuster, and Alan L. Carter
Dryden Flight Research Center

INTRODUCTION

Several operational aircraft have accumulated significant flight time at speeds sufficient to produce severe aerodynamic heating (refs. 1 to 3). Even with this experience, there exists a lack of understanding of how accurately thermal stresses can be predicted on a complex aircraft structure. The ability to predict thermal stresses accurately has great impact on both the safe magnitude of stresses and the long-term effect of thermal cycling on the structure. This paper addresses this deficiency by examining how measured thermal stresses on a laboratory test specimen compare with thermal stresses predicted using a NASA structural analysis (NASTRAN) computer model.

A test structure representing a portion of a hypersonic vehicle (ref. 4) was instrumented with strain gages and thermocouples. This test structure was then subjected to laboratory heating representative of supersonic and hypersonic flight conditions. A finite element computer model of this structure was developed using several types of elements with the NASTRAN program (ref. 5). Temperature inputs from the test were used to predict model thermal stresses, and these were correlated with the test measurements.

DESCRIPTION OF TEST SPECIMEN AND INSTRUMENTATION

A test specimen resulted from work directed toward studying the feasibility of a hypersonic research airplane (ref. 4). One structural concept resulting from this study was a heat sink type of structure. The basic philosophy was to use a variable-thickness, load-carrying skin to absorb heat as required to maintain a certain skin temperature. The skin was supported by a truss-type substructure as shown in figure 1. A beryllium-aluminum composite metal (ref. 6) was selected as

the skin because of the light weight and large thermal capacity of beryllium. The substructure frames were a titanium, truss-type configuration with Ti-6Al-4V being used as the truss material. A photograph of the substructure frames is shown in figure 2. A photograph of the complete specimen is shown in figure 3 where the skins are attached to the substructure.

The location of the temperature and strain instrumentation is shown in figure 4. Eighteen thermocouples and eighteen strain gages were used for analysis purposes in this paper. Eight thermocouples and strain gages were located on the skins, while the remaining ten were located at strategic points on the substructure. Thermocouples and foil-type strain gages were used in the test temperature environment, which ranged from 241° K (-30° F) to 594° K (600° F).

TEST PROCEDURE

The general test setup is shown in the schematic in figure 5. The specimen is completely encased but is supported so that it is unrestrained—in other words, the edges are free to rotate and translate in the plane of the skin. A rack of radiant heaters (ref. 7) is located such that skins can be heated on the side away from the frames. A blower system is situated such that a mixture of air and gaseous nitrogen can be blown over the specimen if cooling is desired.

Two different heating conditions were considered so that a simulation of the heating for both a hypersonic mission and a supersonic mission could be examined. A flight profile for a supersonic cruise airplane is shown in figure 6. This profile is of a 50-minute flight in which more than 30 minutes are spent at a Mach 3 cruise condition. Skin temperatues were calculated based on the computer program identified in reference 8. A flight profile for a hypersonic mission is shown in figure 7. This profile is of a 6-minute rocket-powered mission (ref. 4) with a 1-minute cruise at Mach 6. Skin temperatures were also calculated for this flight profile.

Time histories of skin temperatures for the two profiles were used to perform the test. In the case of the supersonic profile, the test began at room temperature with radiant heating of the skins to the prescribed flight profile. At the end of the thirty-plus minutes at the Mach 3 temperatures, cold gaseous nitrogen and air were blown over the specimen to simulate the cooling effect which occurs during descent. In the case of the hypersonic profile, the test specimen is cooled prior to heating to simulate the cold soak condition that occurs when rocket-powered aircraft are air launched at high altitude. After the specimen is cooled, the heating is started by controlling the skin temperatues with radiant heaters according to the prescribed temperature time history.

DESCRIPTION OF THE NASTRAN MODEL

A 237-element NASTRAN model of the test component was developed for one of the symmetrical quarters of the structure as shown in figure 8. The model, which

had a surface area of 0.34 square meter (3.68 square feet) and a nominal depth of 0.10 meter (4 inches), was identified as TITRUS and composed of bar, rod, and shear panel elements. There were 96 grid points with 131 bars, 40 rods, and 66 shear panels. The skins were modeled with bar elements and shear panels (fig. 9). The truss frames were modeled as bar elements, rod elements, and shear panels. Twenty-one single-point constraints were utilized to appropriately control the displacements and rotations at the edges of the model. Thirty-eight multiple-point constraints were utilized with respect to the rods to prevent them from collapsing. The model had 475 degrees of freedom, and 592 bulk data cards were used. The correlation of the instrumentation locations to structural model elements is shown in figure 10. The grid point numbering system for the NASTRAN model is shown in figure 11.

RESULTS

The results of the supersonic and hypersonic heating simulations are presented in figures 12 and 13, respectively. Time histories of temperatures and thermal stresses resulting from the tests are represented by the solid lines. Thermal stresses calculated using the NASTRAN model are represented by the circular symbols.

Temperatures for the supersonic heating simulation begin near room temperature for the entire structure. The skins reach a maximum temperature near 515° K (460° F) while the substructure remains significantly cooler. These temperature changes and variations induce the measured thermal stresses that are presented. It can be seen that the skin thermal stresses (F, G, H, I, J, K, L, and M) are relatively small and may be either in tension or compression. The very large thermal stresses occur in the upper caps (E and N) where large tensile values occur. The lower cap thermal stresses (A, B, C, P, Q, and R) were generally small as were the truss link stresses (D and O). Strain gages C and D exhibited erratic behavior, which was assumed to indicate a sensor failure.

Temperatures for the hypersonic heating simulation begin near 241° K (-30° F) for the entire structure. Since previous hypersonic research aircraft are rocket powered, they are usually air launched from another aircraft to gain an altitude advantage. This very cold initial temperature soak represents the cold soak occurring at high altitude prior to air launching. The skins reach a maximum temperature near 594° K (600° F) while the substructure remains considerably cooler. The thermal stresses, in general, follow the same pattern as was observed for the supersonic case. The very large stresses again occurred in the upper caps (E and N). The stresses, in general, were larger for the hypersonic case, as would be expected for larger thermal gradients. Strain gage D exhibited erratic behavior, so it was assumed to have failed.

Thermal stresses calculated using the NASTRAN model with temperature inputs from the heating simulation are presented as the circular symbols. Most of the NASTRAN elements correspond to a strain gage location and therefore the thermal stresses can be compared directly. There are several cases, such as element number 2083, which should correspond more closely to the average of strain gages A and B because the model was not broken up into more elements at that particular location. The same comment is applicable for elements 2078, 2033, and 2038.

DISCUSSION

The primary purpose of this paper is to determine how well thermal stress can be predicted using a NASTRAN computer model. The basic comparison is made by examining the content of figures 12 and 13. The experimentally measured thermal stresses are directly compared to thermal stresses calculated using the previously described NASTRAN model. It is logical to discuss the comparisons in four distinct areas of the structural component: the lower cap area, the truss links, the upper cap area, and the skins. The upper cap is the area closest to the skins, while the lower cap area is the farthest from the skins.

Strain gages A, B, C, P, Q, and R are located in the lower cap area (fig. 10). Elements 2033, 2038, 2078, and 2083 are associated with the foregoing strain sensors. The following strain gages/elements are directly comparable: A/2083, C/2078, P/2033, and R/2038. The average of elements 2078 and 2083 would come the closest for comparison to strain gage Q.

The hypersonic heating simulation was conducted prior to the supersonic heating simulation. Strain gage C failed before the supersonic heating test could be completed; hence, there are no data for strain gage C. In general, the skin thermal stresses were predicted quite well (for both the supersonic and hypersonic simulations). Strain gages A, C, and P (figs. 12 and 13) correlated very well with the thermal stresses calculated from the NASTRAN model. Strain gages B and Q could not be directly compared to one specific NASTRAN element; however, the measured thermal stresses appeared to be in the expected range when they were compared to the elements in close proximity (B/2078 and 2083, Q/2033 and 2038). Strain gage R (fig. 13(d)) did not agree with the NASTRAN predictions at all for the hypersonic test. The measured thermal stresses were several times larger than those predicted by the NASTRAN model. The data for strain gage R correlated much better for the supersonic case (fig. 12(c)).

There were only two strain gages on the truss links, and one (strain gage D) failed during the test. Only strain gage O was operative on the truss links. The truss link thermal stresses were measured as very small quantities, and this was substantiated by the NASTRAN model (figs. 12(f) and 13(g)).

Large thermal stresses occurred throughout both the supersonic and hypersonic heating tests for strain gages E and N (figs. 12(g), 12(h), 13(h), and 13(i)). It can be seen that the NASTRAN calculated thermal stresses exceeded the measured stresses significantly for the supersonic case. Particularly, the thermal stress calculated at location N was 30 to 40 percent above the measured thermal stresses. The other cases showed better agreement with the thermal stresses calculated at location N, being quite comparable to the measured data for the hypersonic heating.

Locations F, G, H, I, J, K, L, and M are skin sensors which are presented in figures 12(f) to 12(p) and 13(g) to 13(j). The thermal stresses calculated at locations K, L, J, I, and G compared closely to measured thermal stresses for the supersonic heating test (fig. 12). The thermal stresses measured at locations M, H,

and F did not compare closely to the NASTRAN calculations. Strain gages M and N are both located in the center of the panel; hence, their locations are geometrically similar. The time histories are also very similar in that the NASTRAN model indicates a small compressive stress at these locations while the test data show a small tensile stress throughout the majority of the time history. The calculated thermal stresses at location F are considerably larger than the measurements.

The skin thermal stresses for the hypersonic heating simulation yielded similar results. The calculated thermal stresses at locations K, L, M, J, I, and G compared closely to measured thermal stresses (fig. 13). The thermal stresses at H and F did not compare closely to the NASTRAN calculations. The calculated thermal stresses at location H were fairly large compressive stresses while the measured thermal stresses were close to zero. The NASTRAN model indicated some very large tensile stresses at location F which were not substantiated by test measurements.

The data presented in figures 12 and 13 can be examined in a more informative manner. The distribution of temperature for an instant in time (time = 12 minutes) for the supersonic case is presented in figure 14. The temperature distribution on the left is for the left spar, and the distribution to the right is for the right spar. The temperature distribution at the bottom is for the skin. Thermal stress distributions corresponding to the figure 14 temperature distributions are shown in figure 15 for the 12-minute time segment. It can be seen that the distribution predicted using the NASTRAN model correlates closely with the thermal stresses measured during the test.

The temperature distribution shown in figure 16 is at the 4-minute time segment of the hypersonic heating profile. Thermal stress distributions corresponding to the figure 16 temperature distributions are shown in figure 17. The distribution of thermal stress resulting from the NASTRAN model correlates closely with the thermal stresses measured during the hypersonic heating test.

CONCLUDING REMARKS

There are two very important issues that have been addressed in this paper. The first is to assess how well a NASTRAN model can predict thermal stress distributions and time histories of thermal stress in a complex structure. The second is to provide a level of experience from which estimates of required model complexities can be obtained with respect to temperature input requirements, resulting thermal stresses, and type of structural elements.

The NASTRAN model, in general, predicted the thermal stresses measured during laboratory simulated supersonic and hypersonic heating conditions very well for approximately 70 percent of the structural elements which were examined. There were significant, although not necessarily unexpected, discrepancies for approximately 30 percent of the structural elements considered.

The NASTRAN model was developed with 237 bar, rod, and shear panel elements. The model contained approximately 700 elements per square meter (65 elements

per square foot) of surface area. This element density was considered adequate to predict the distribution of thermal stress and the time histories of thermal stress reliably. Approximately 280 temperature inputs per square meter (26 per square foot) of surface area were required to develop predicted thermal stresses.

Dryden Flight Research Center
National Aeronautics and Space Administration
Edwards, Calif., October 19, 1978

REFERENCES

1. Quinn, Robert D.; and Olinger, Frank V. (appendix A by James C. Dunavant and Robert L. Stallings, Jr.): Heat-Transfer Measurements Obtained on the X-15 Airplane Including Correlations With Wind-Tunnel Results. NASA TM X-1705, 1969.

2. Andrews, William H.: Summary of Preliminary Data Derived From the XB-70 Airplanes. NASA TM X-1240, 1966.

3. Quinn, Robert D.; and Olinger, Frank V.: Flight Temperatures and Thermal Simulation Requirements. NASA YF-12 Flight Loads Program, NASA TM X-3061, 1974, pp. 145-183.

4. Combs, H. G., et al.: Configuration Development Study of the X-24C Hypersonic Research Airplane - Executive Summary. NASA CR 145274, 1977.

5. McCormick, Caleb W., ed.: The NASTRAN User's Manual (Level 15). NASA SP-222(01), 1972.

6. Aerospace Structural Metals Handbook. Volume 4 - Non-Ferrous Alloys. AFML-TR-68-115, Air Force Materials Lab., Wright-Patterson AFB, 1978.

7. Sefic, Walter J.; and Anderson, Karl F.: NASA High Temperature Loads Calibration Laboratory. NASA TM X-1868, 1969.

8. Gord, P. R.: Measured and Calculated Structural Temperature Data From Two X-15 Airplane Flights With Extreme Aerodynamic Heating Conditions. NASA TM X-1358, 1967.

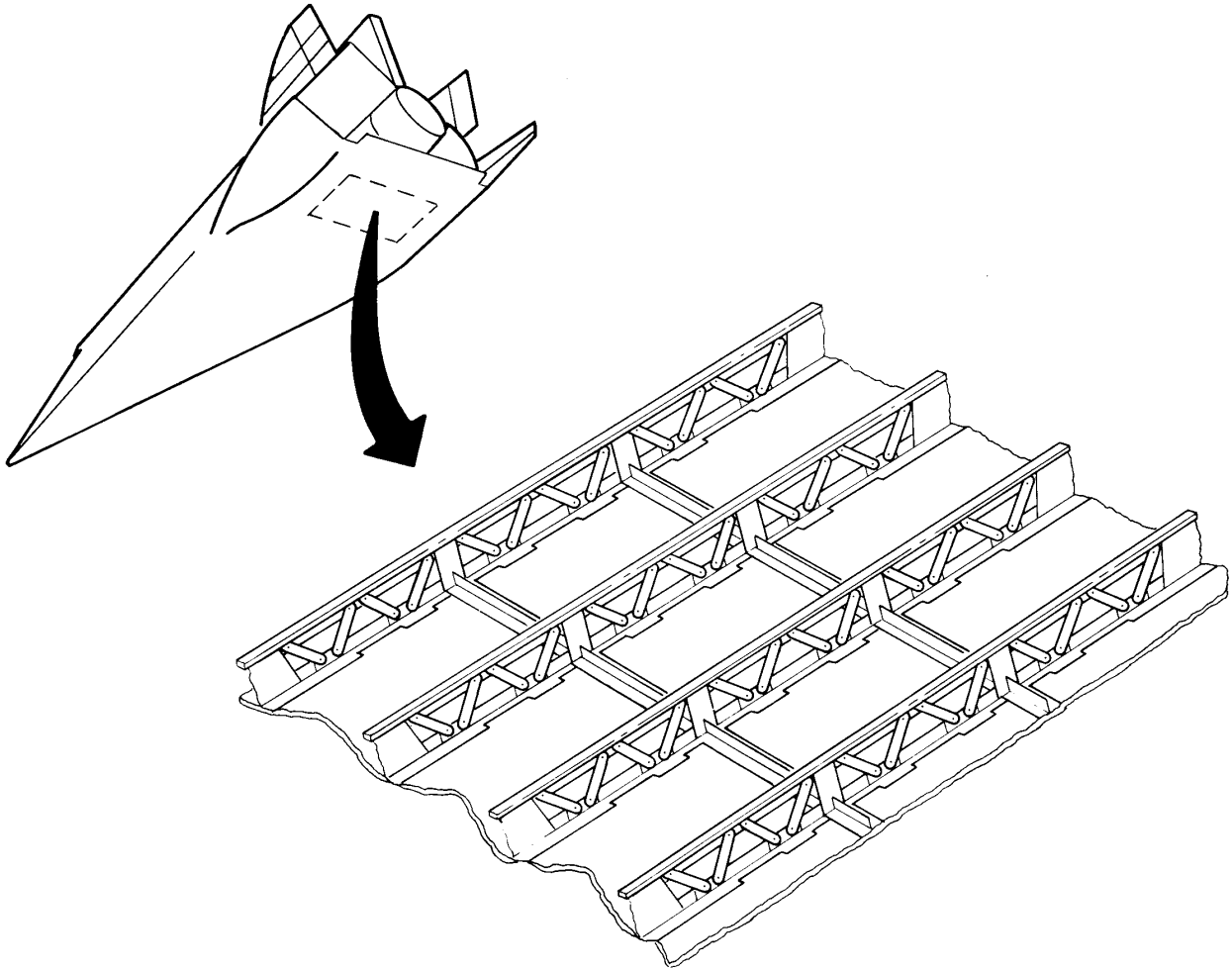

Figure 1. Location of test specimen on hypothetical hypersonic airplane.

E-31365

Figure 2. Titanium truss substructure frames.

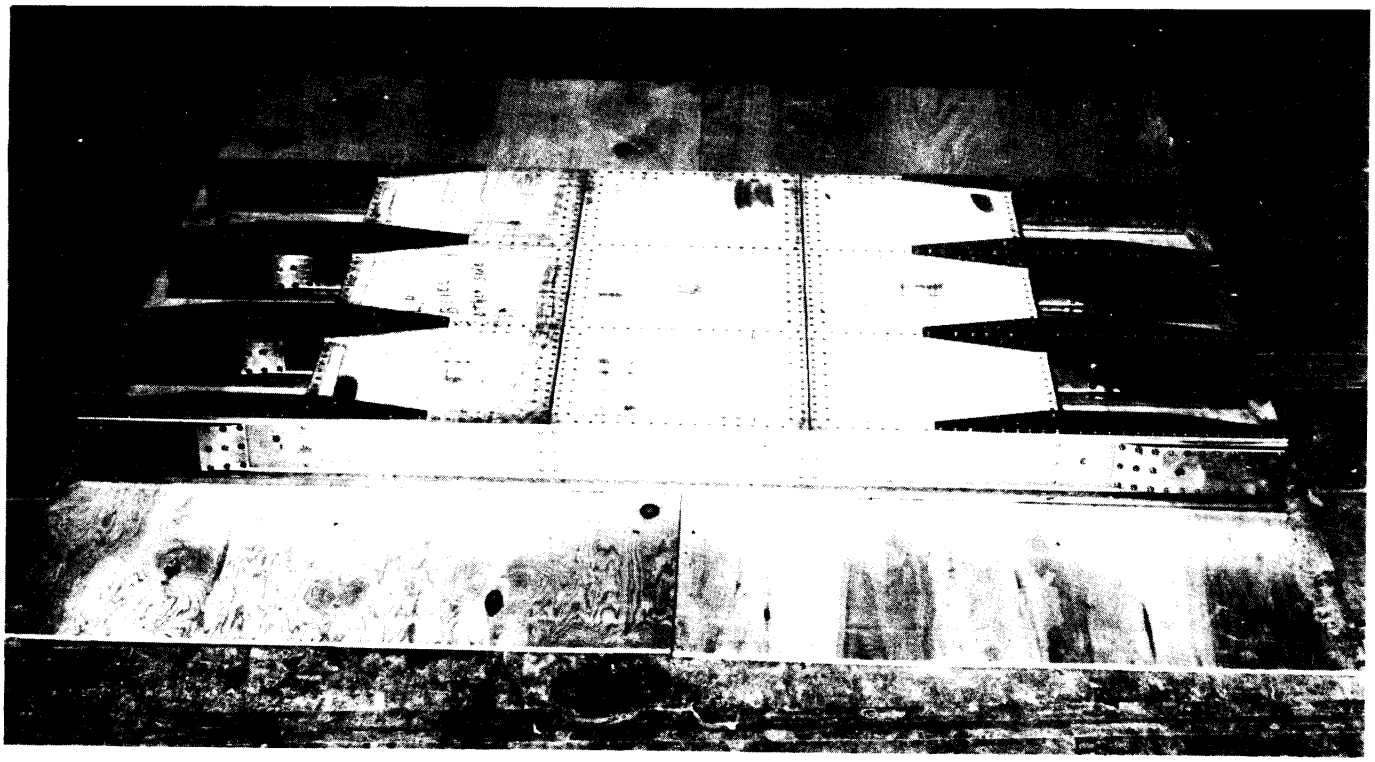

E-31364

Figure 3. Titanium truss/beryllium-aluminum skin test component.

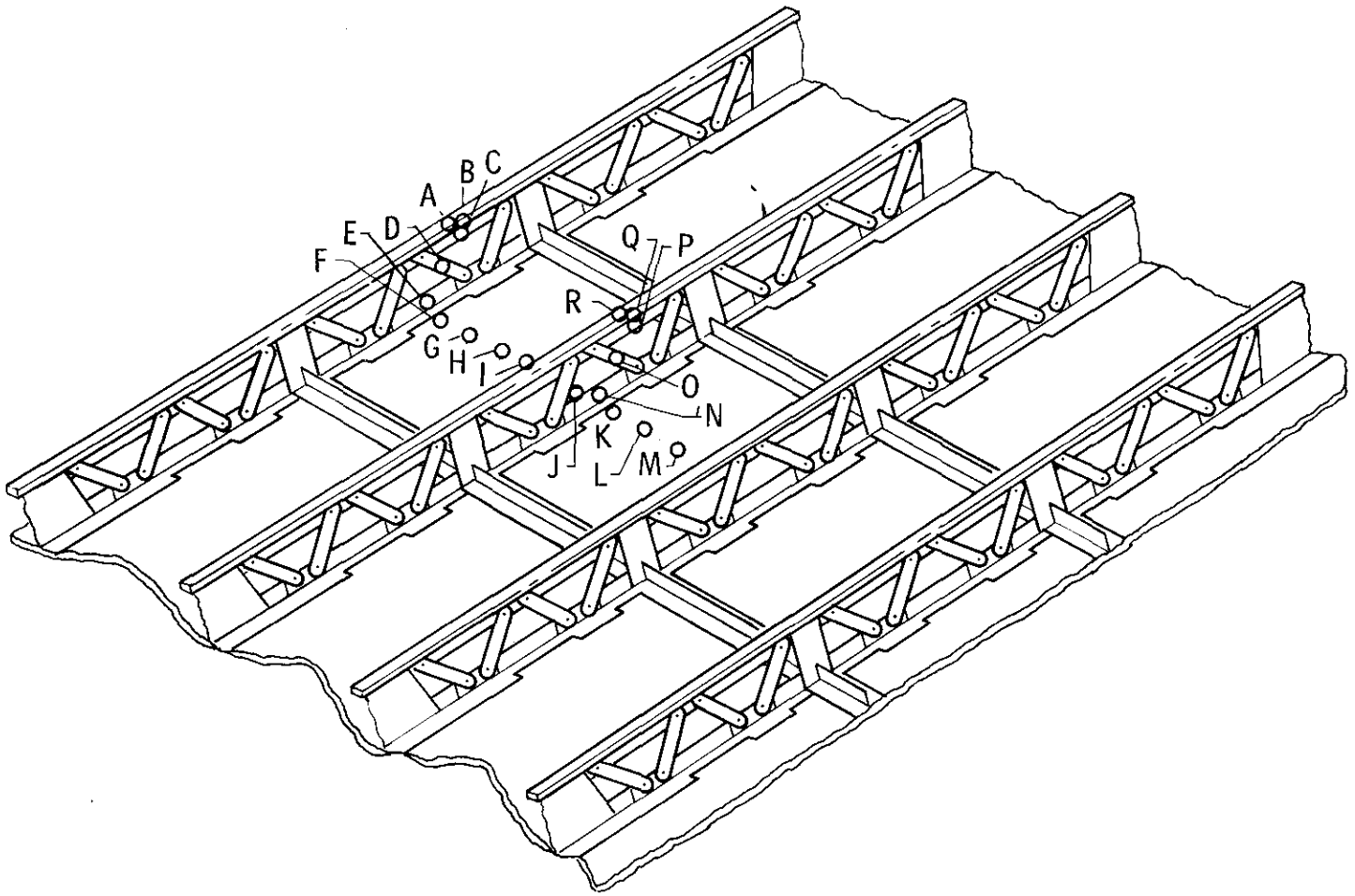

Figure 4. Location of strain gages and thermocouples used for analysis.

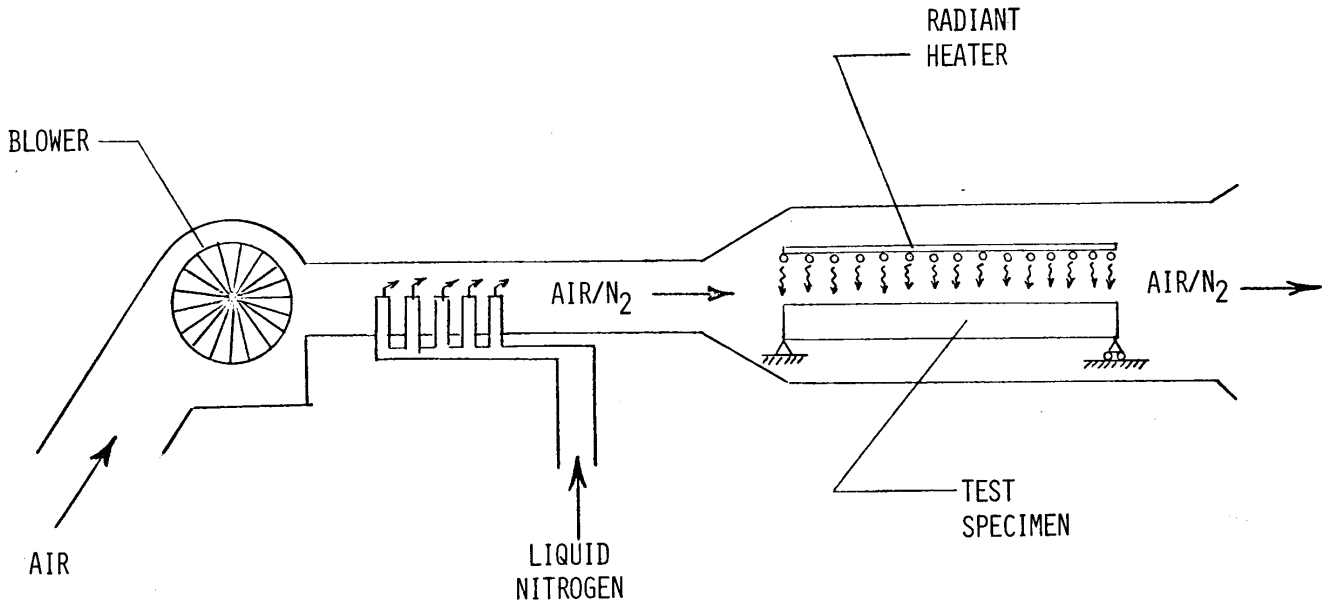

Figure 5. Schematic illustrating the general test setup.

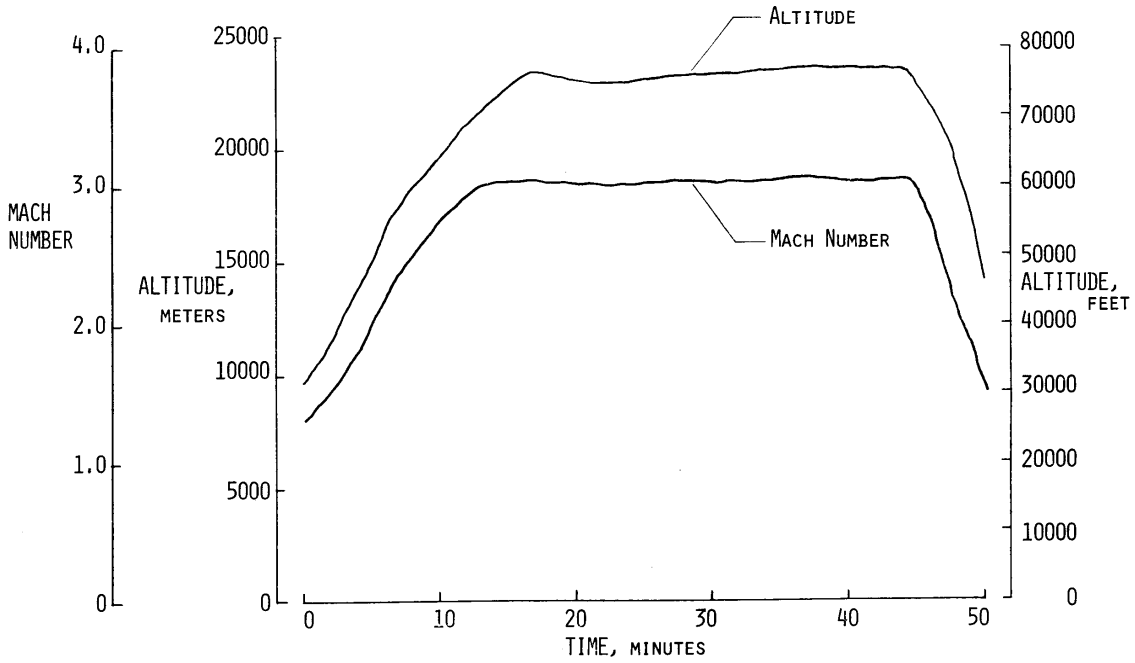

Figure 6. Time history of altitude and Mach number for a supersonic flight.

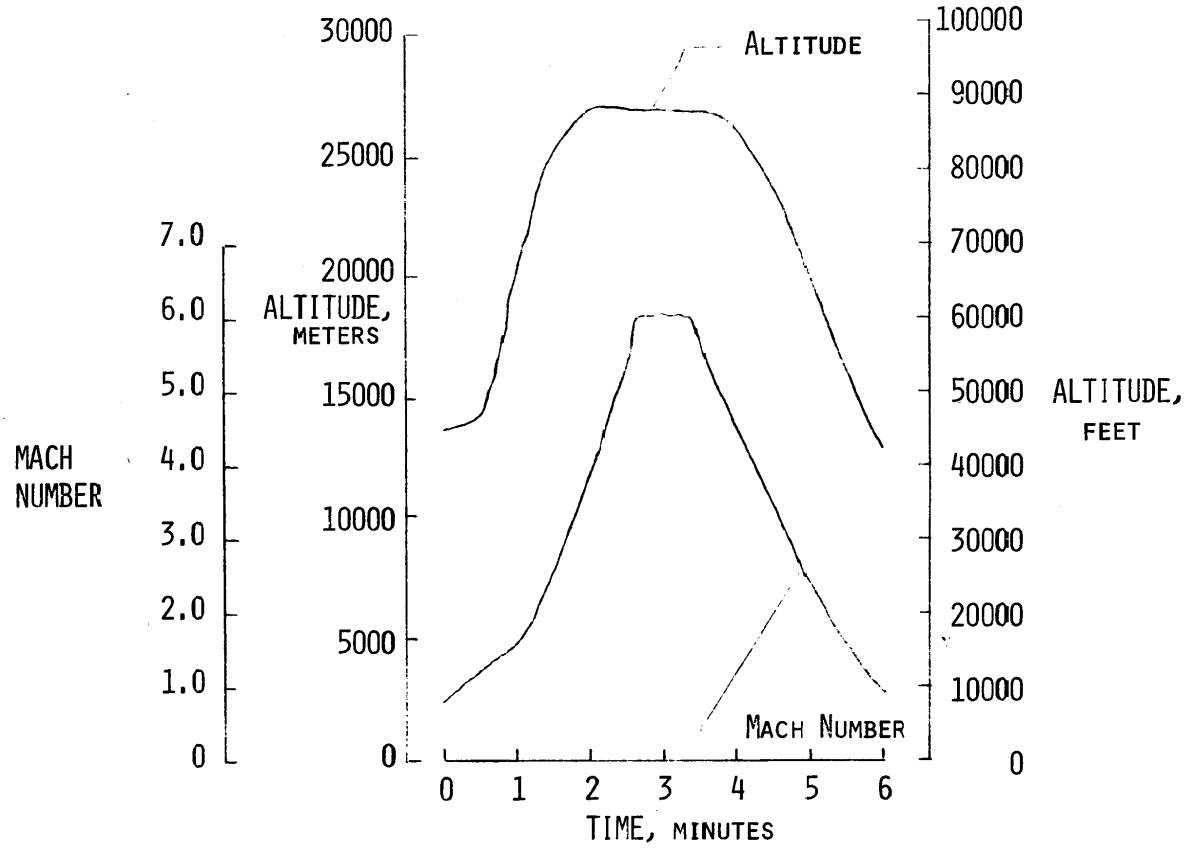

Figure 7. Time history of altitude and Mach number for a hypersonic flight.

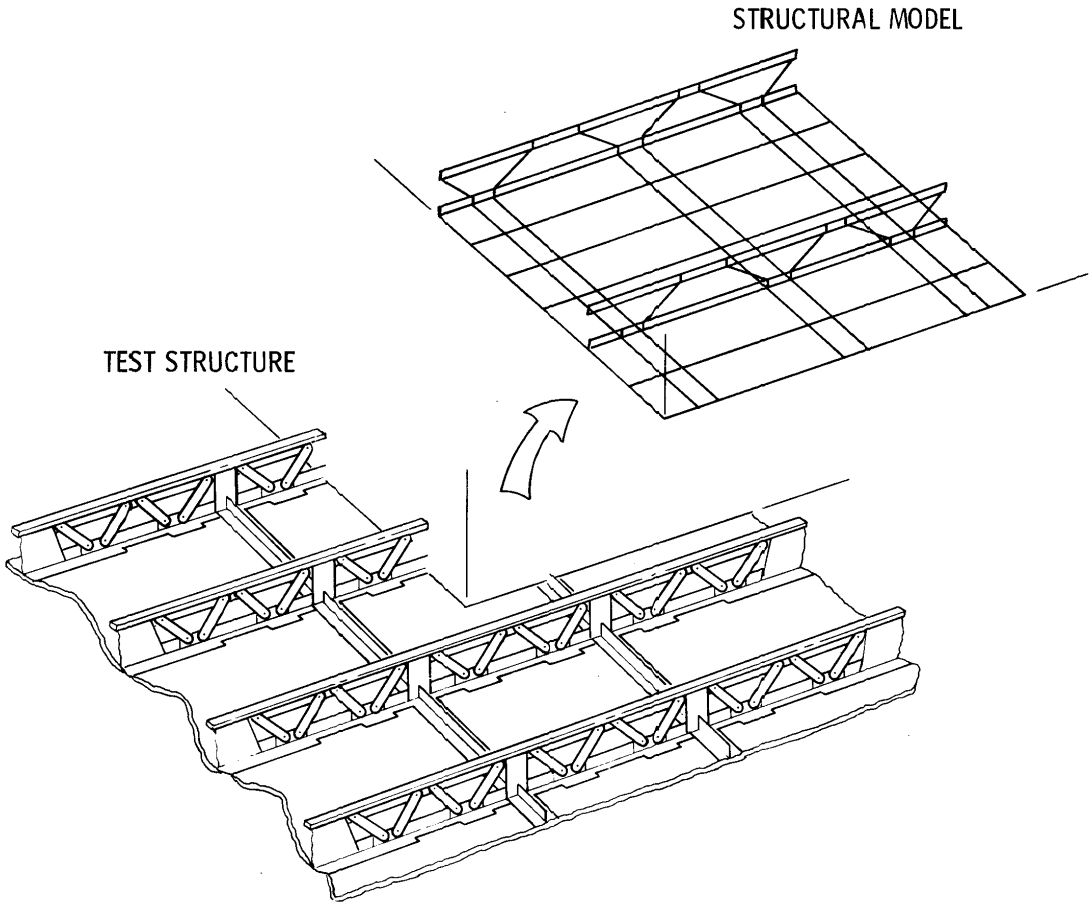

Figure 8. Test structure showing location of structural model.

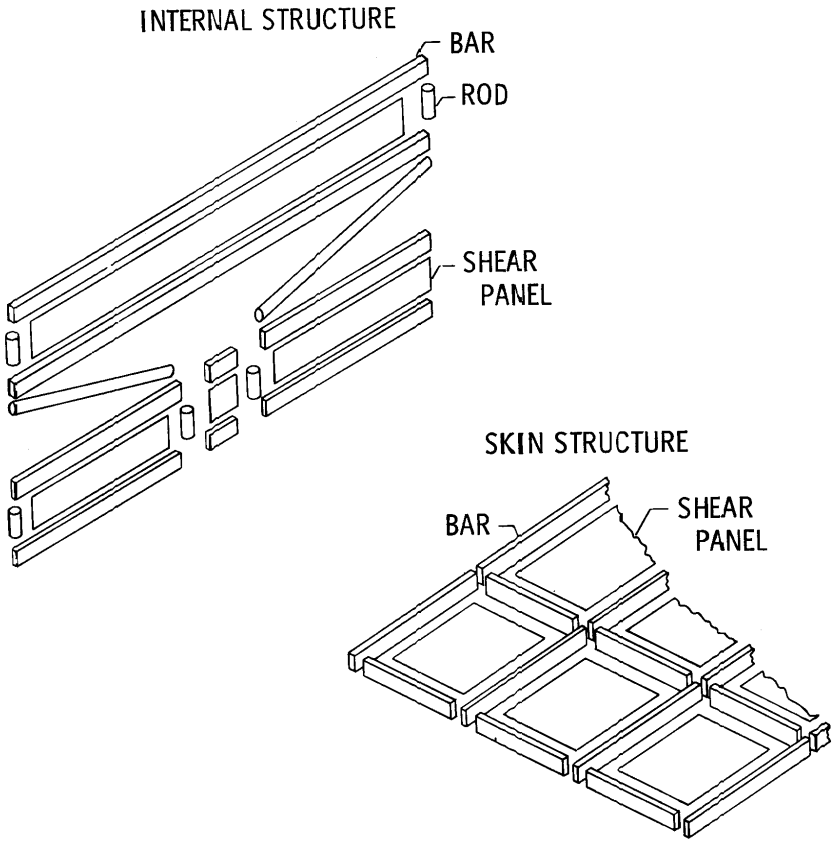

Figure 9. Details of structural model TITRUS.

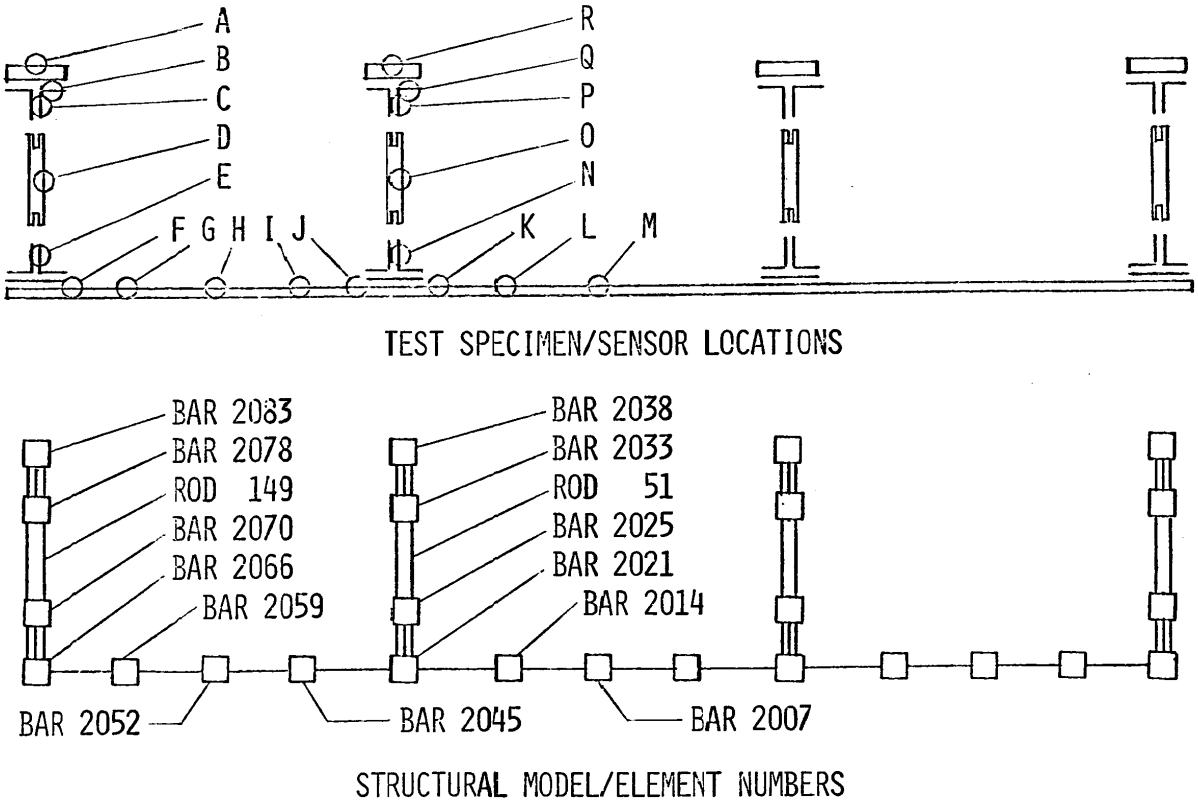

Figure 10. Correlation of test specimen sensor locations with structural model elements.

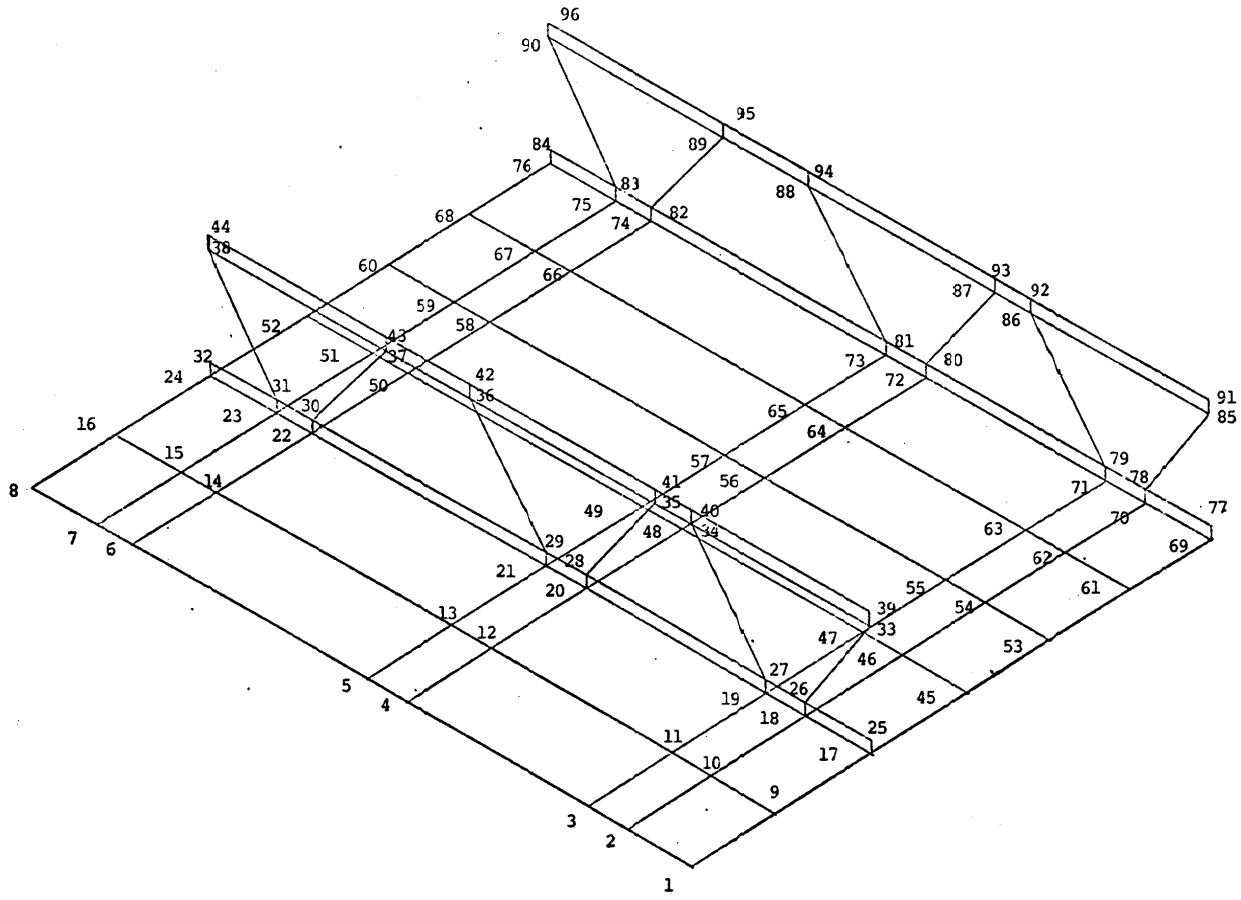

Figure 11. Grid point numbering system for NASTRAN model.

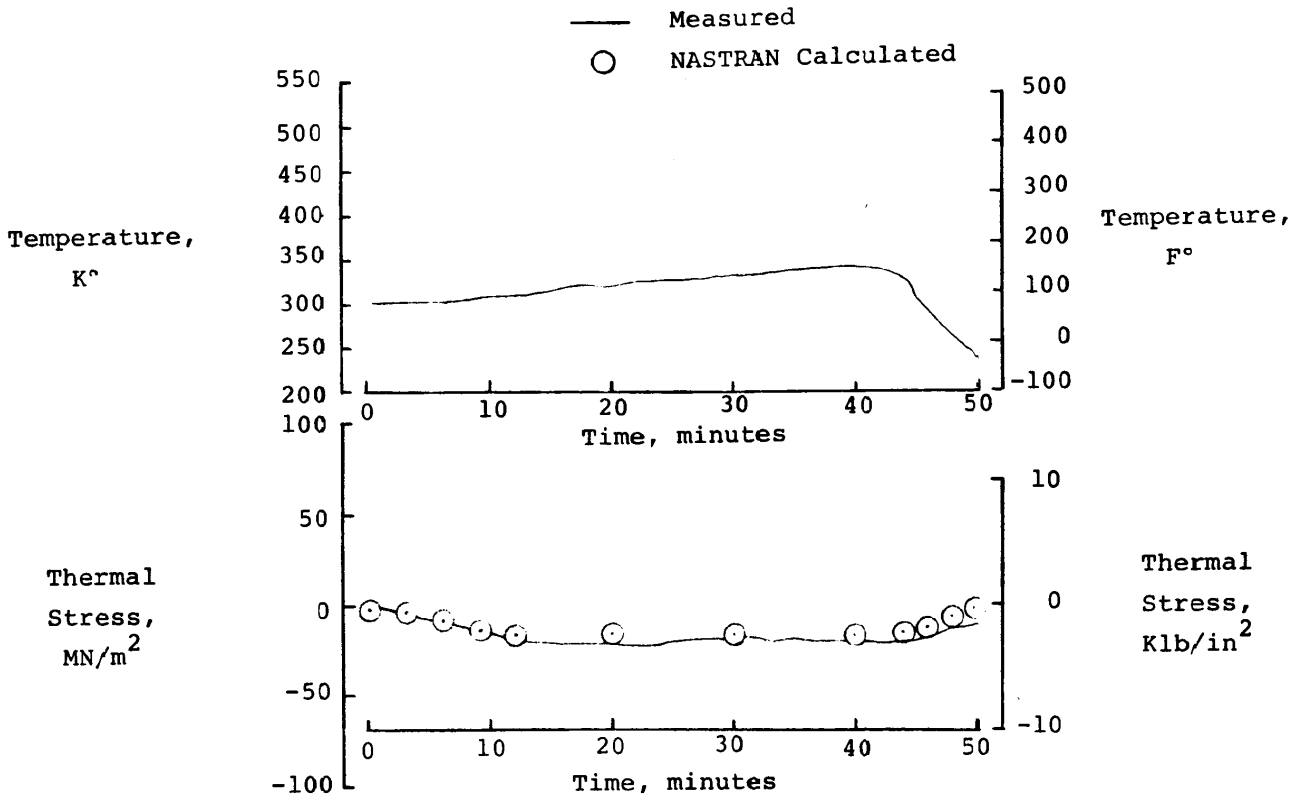

(a) Location A.

Figure 12. Measured temperatures and comparison of measured and NASTRAN-calculated thermal stresses for supersonic heating simulation.

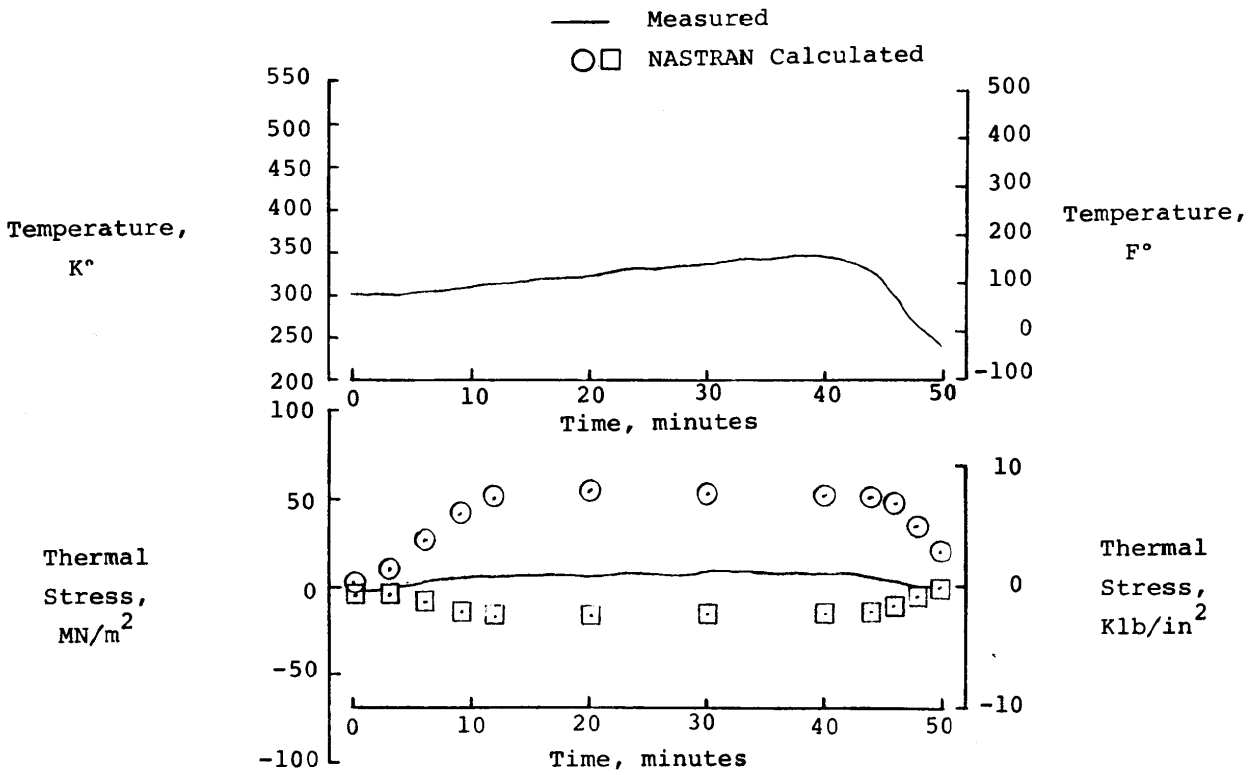

(b) Location B.

Figure 12. Continued.

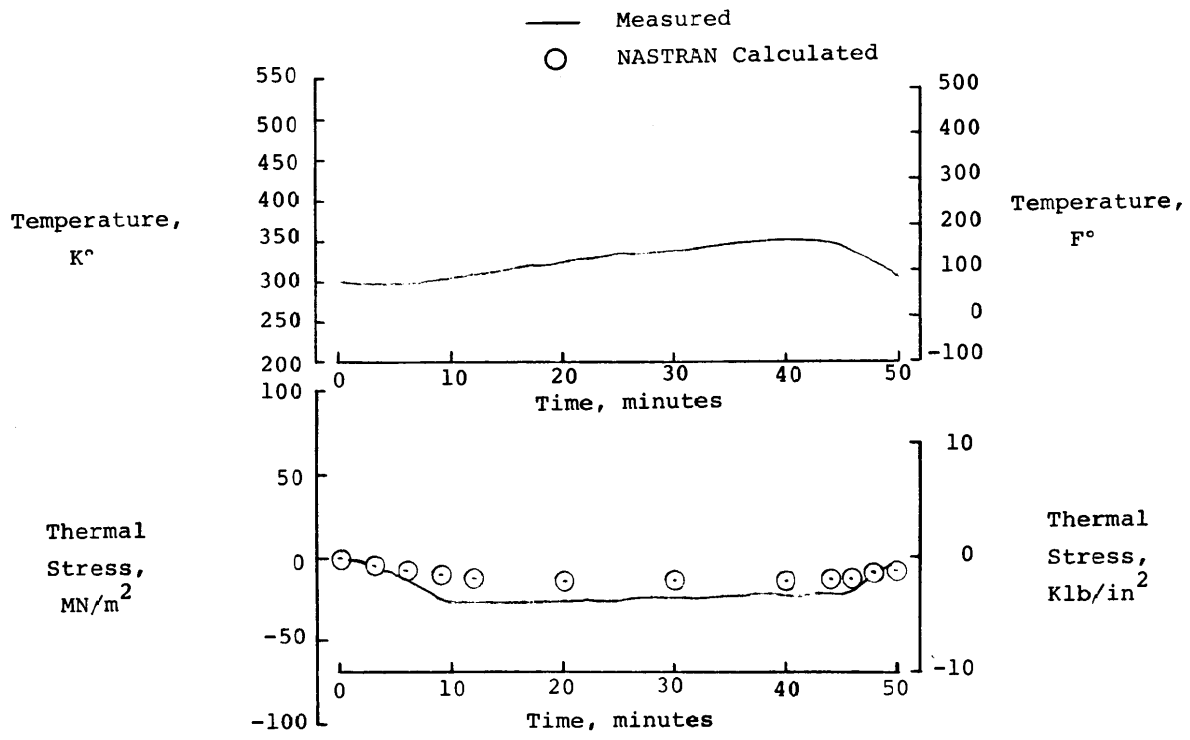

(c) Location R.

Figure 12. Continued.

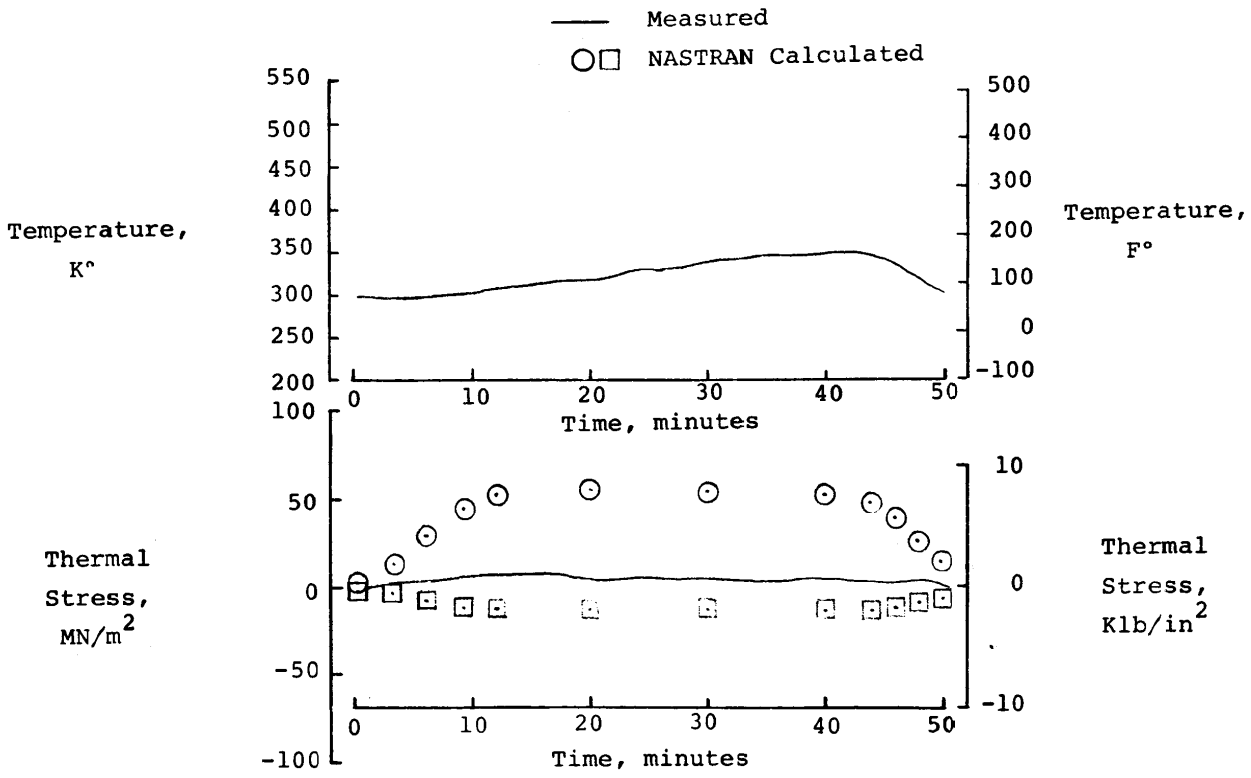

(d) Location Q.

Figure 12. Continued.

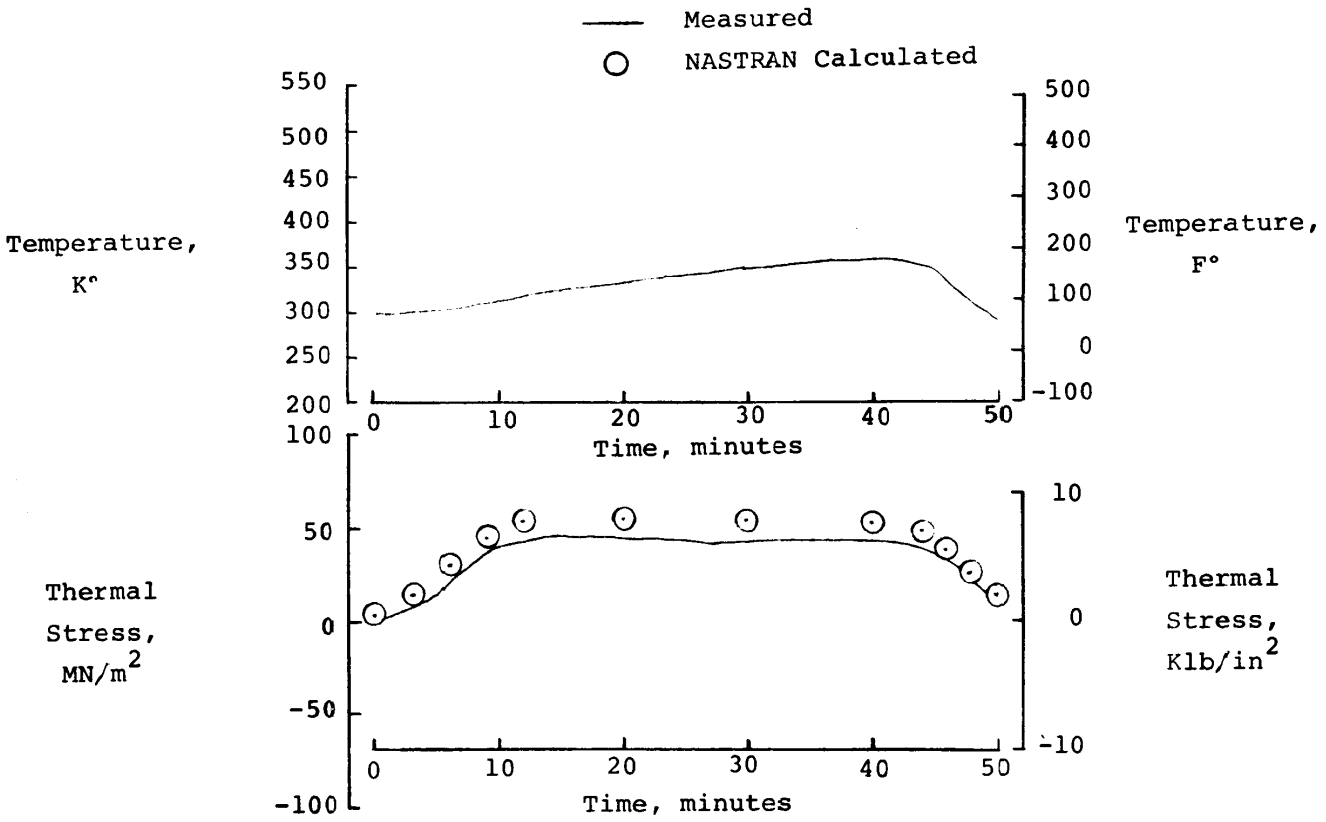

(e) Location P.

Figure 12. Continued.

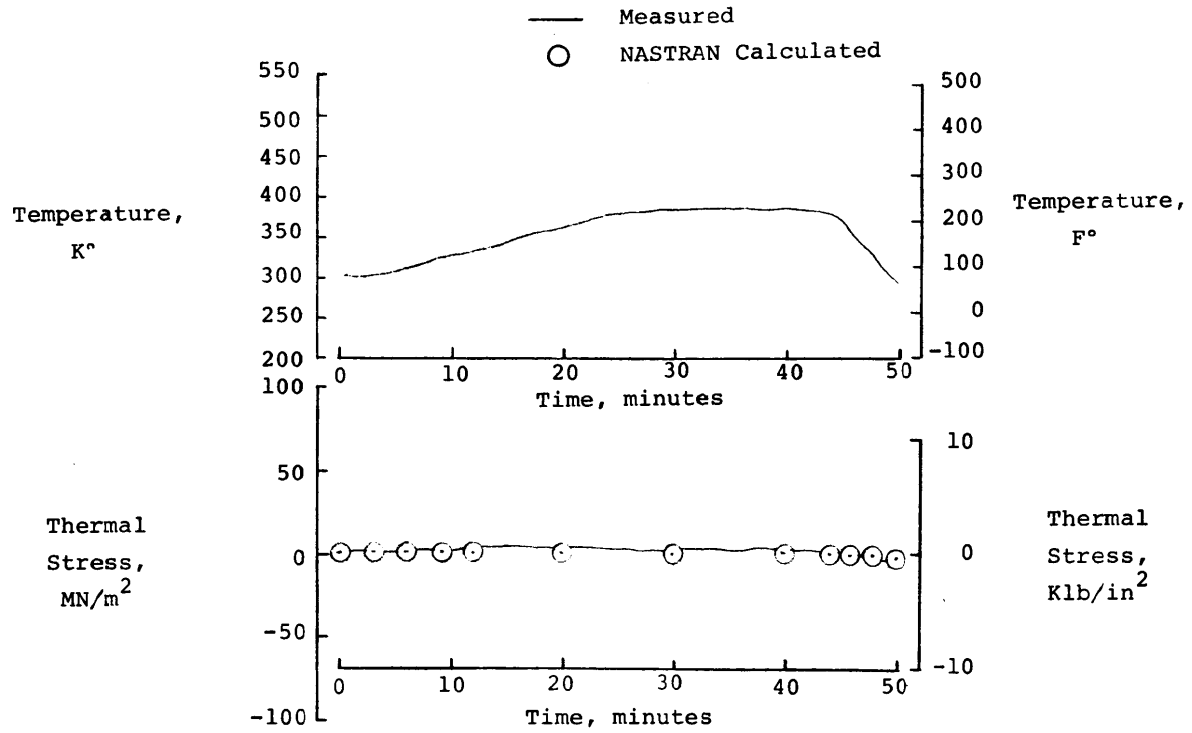

(f) Location O.

Figure 12. Continued.

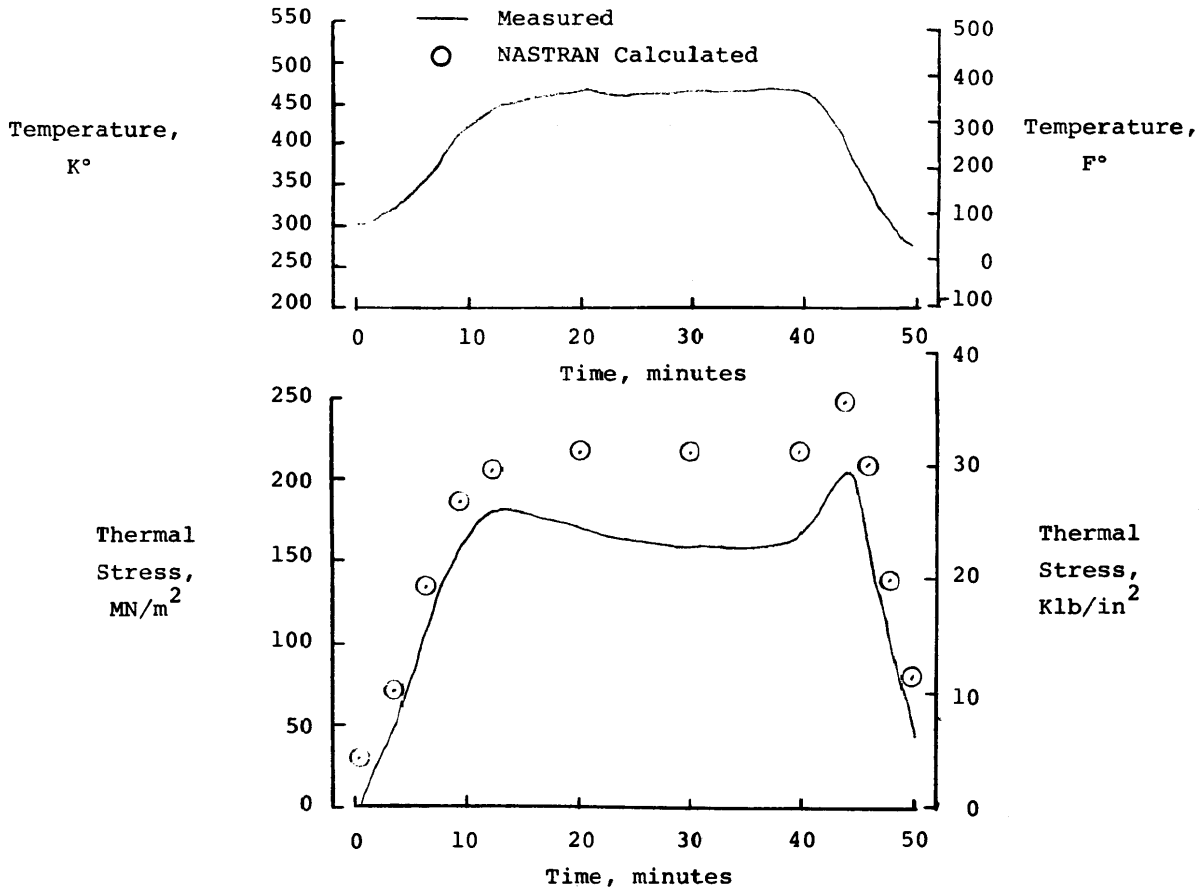

(g) Location E.

Figure 12. Continued.

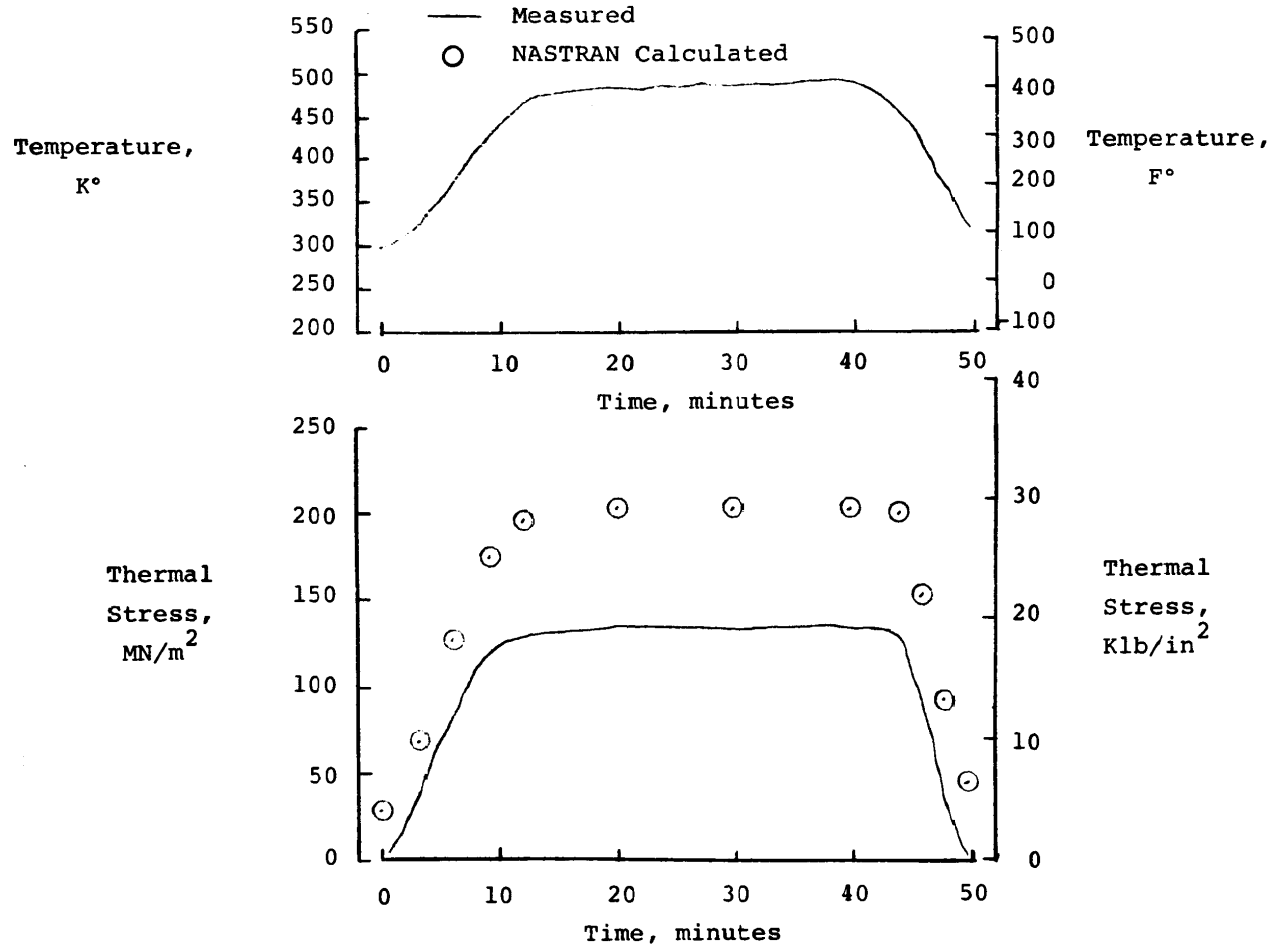

(h) Location N.

Figure 12. Continued.

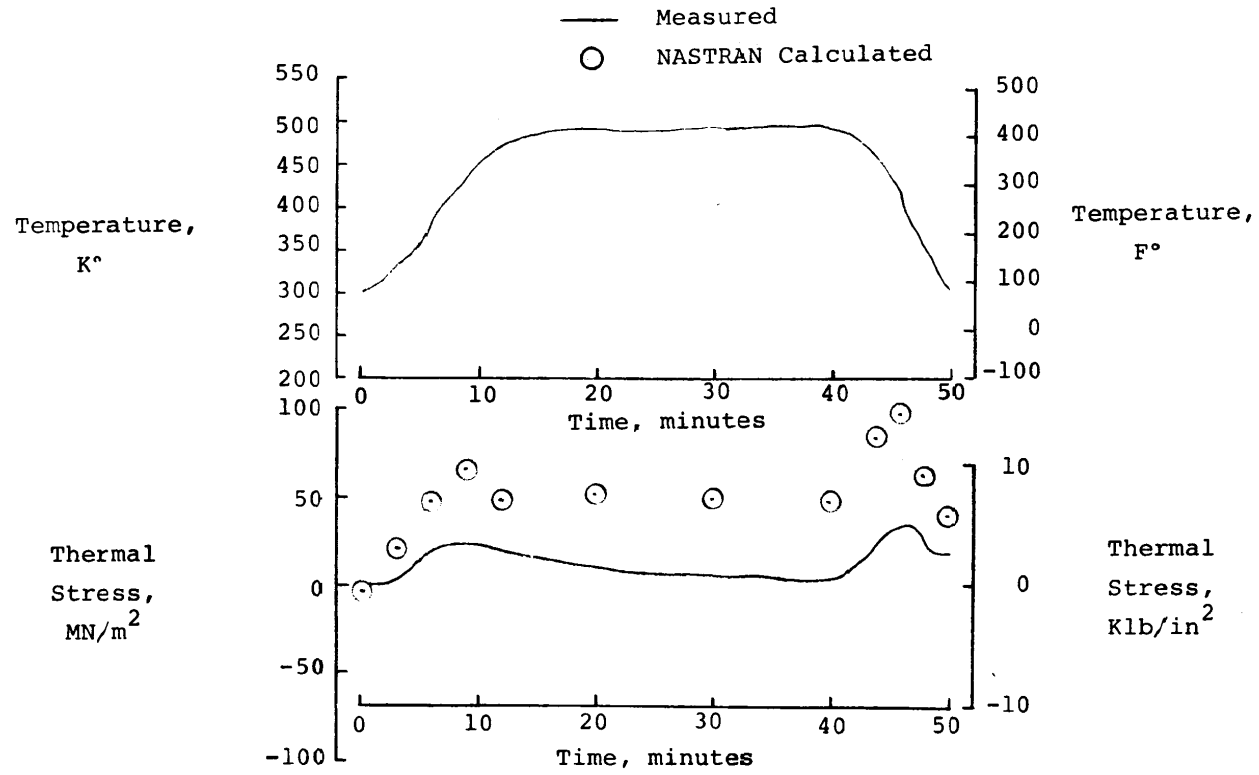

(i) Location F.

Figure 12. Continued.

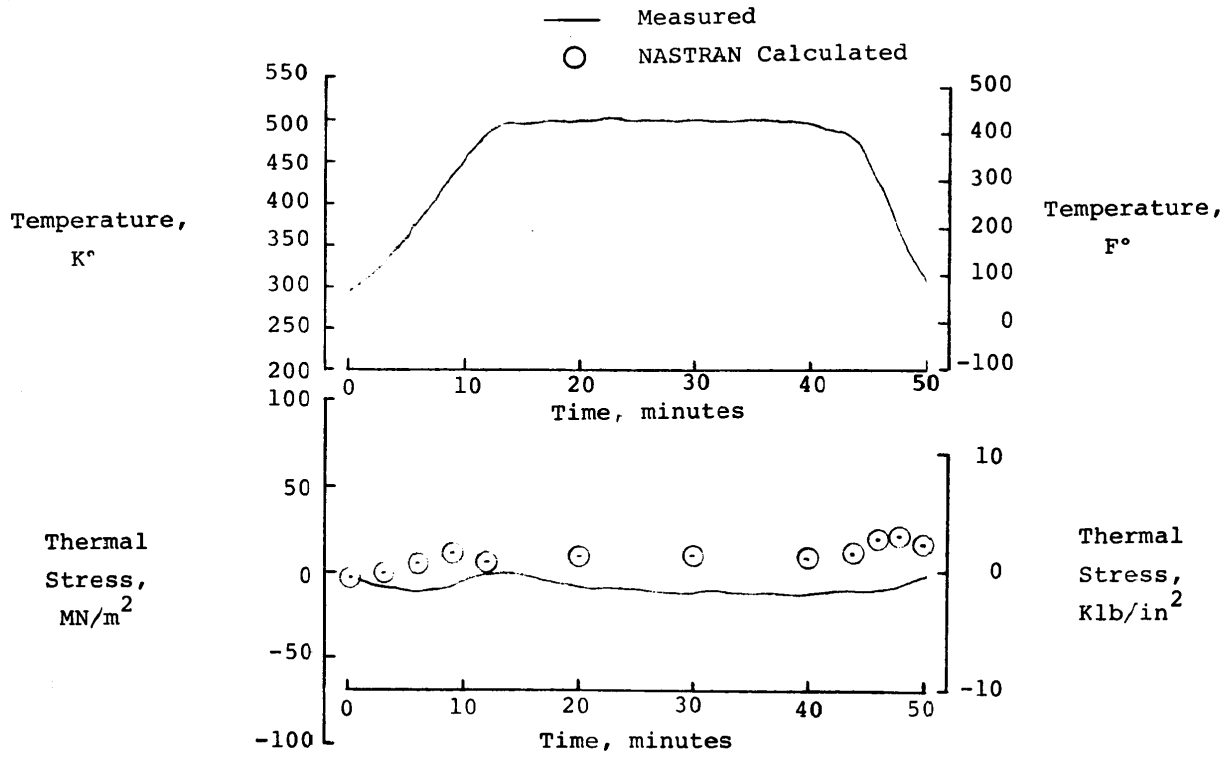

(j) Location G.

Figure 12. Continued.

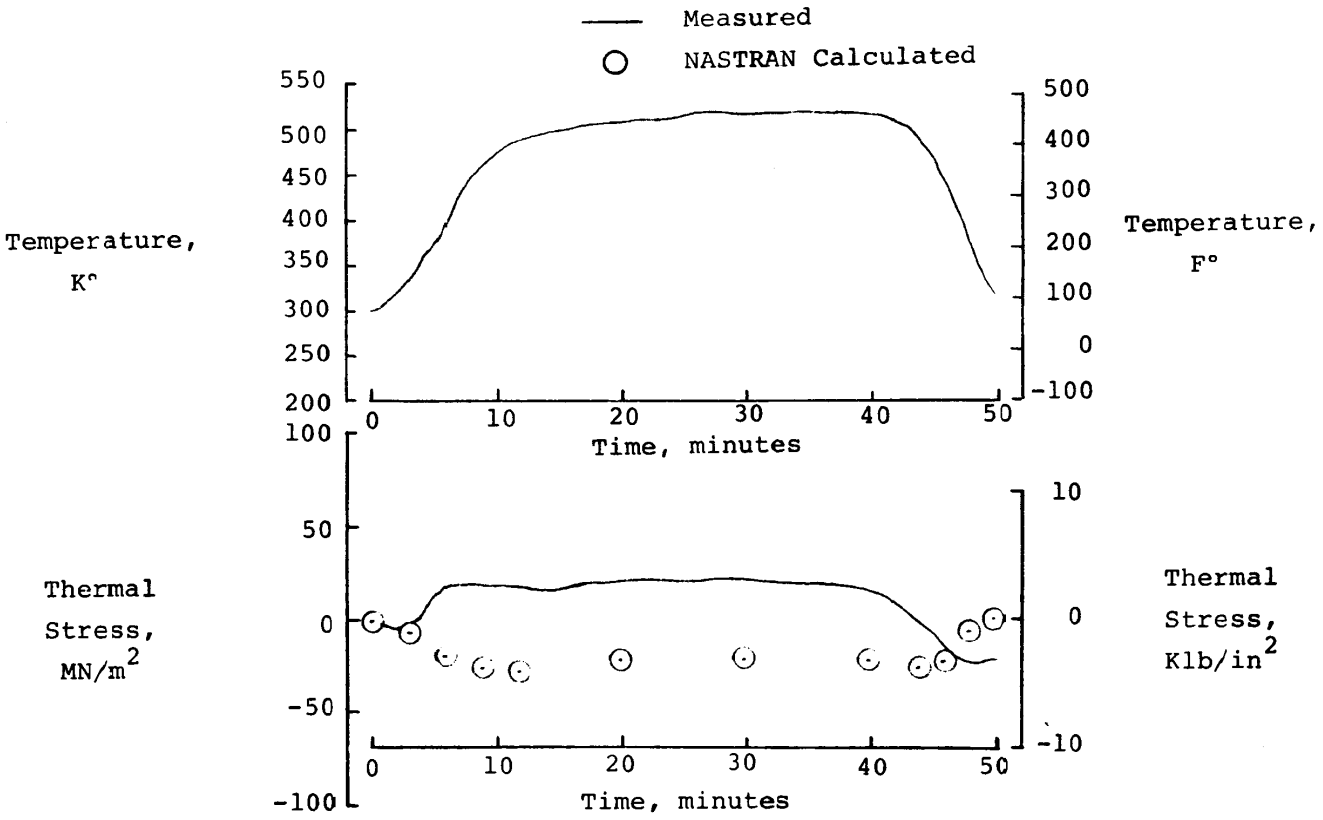

(k) Location H.

Figure 12. Continued.

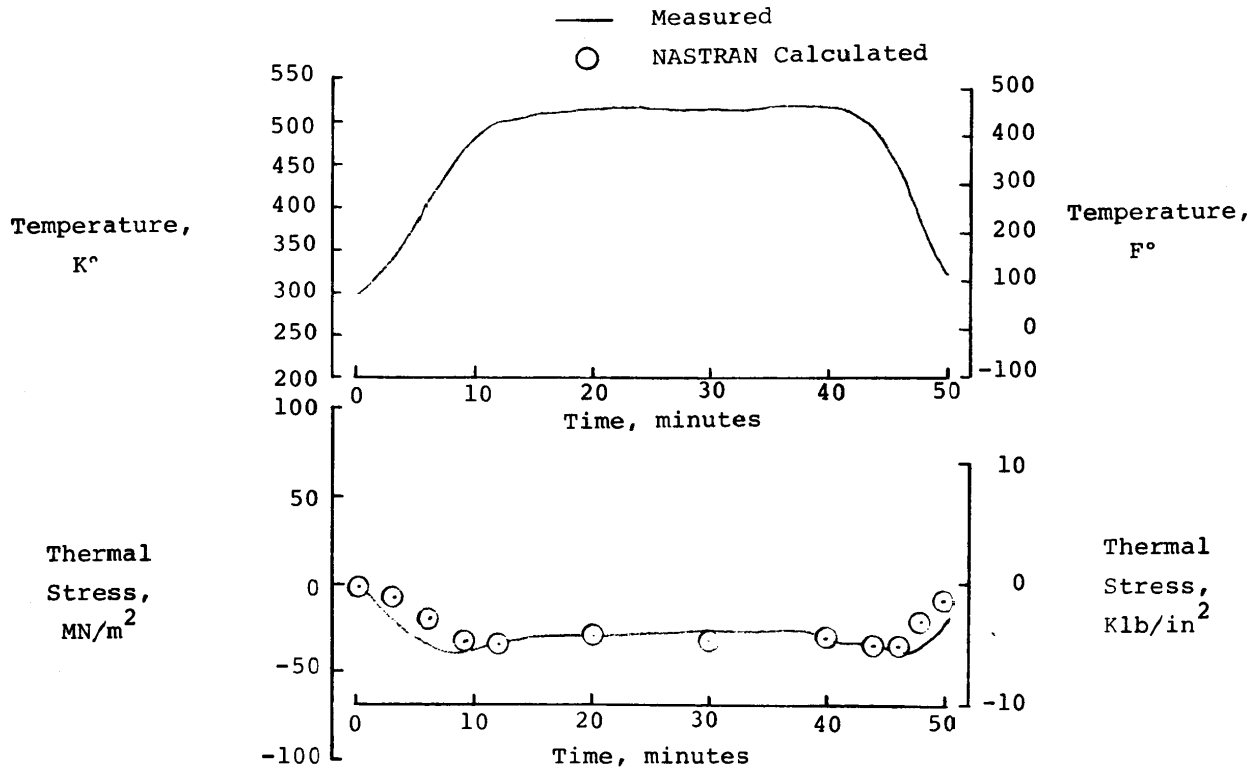

(l) Location I.

Figure 12. Continued.

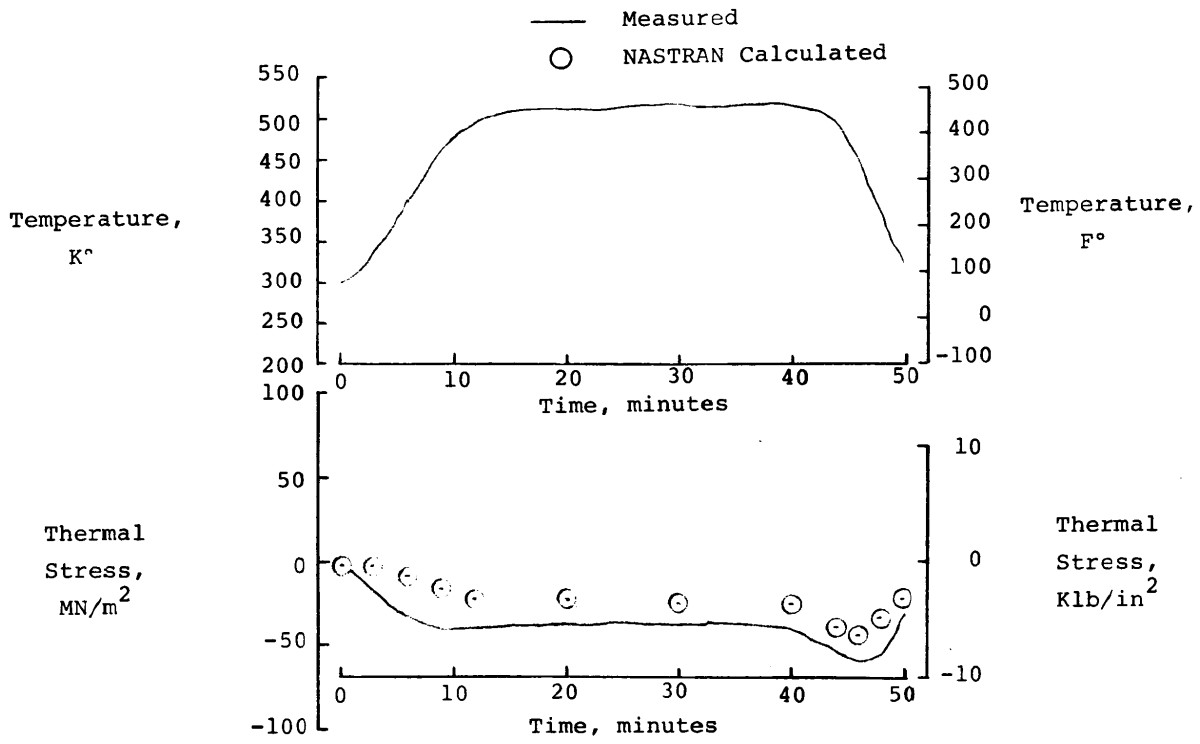

(m) Location J.

Figure 12. Continued.

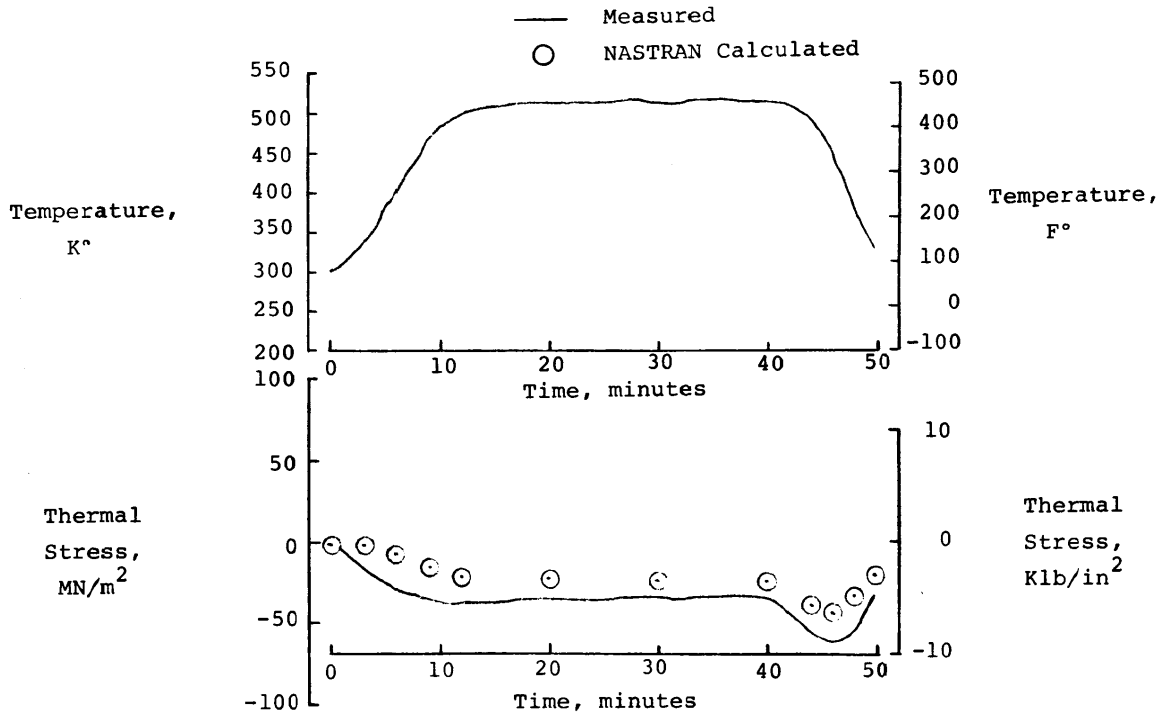

(n) Location K.

Figure 12. Continued.

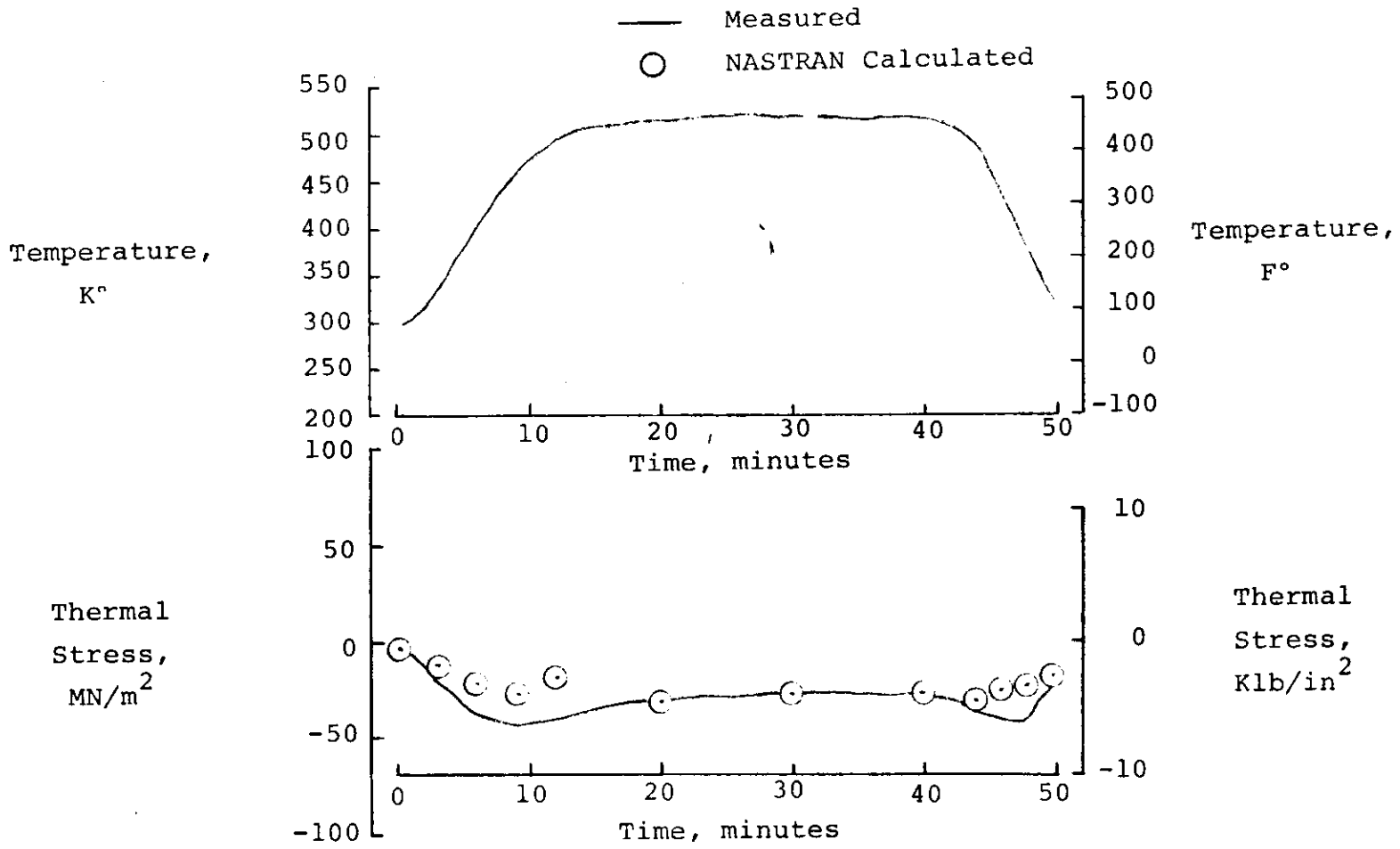

(o) Location L.

Figure 12. Continued.

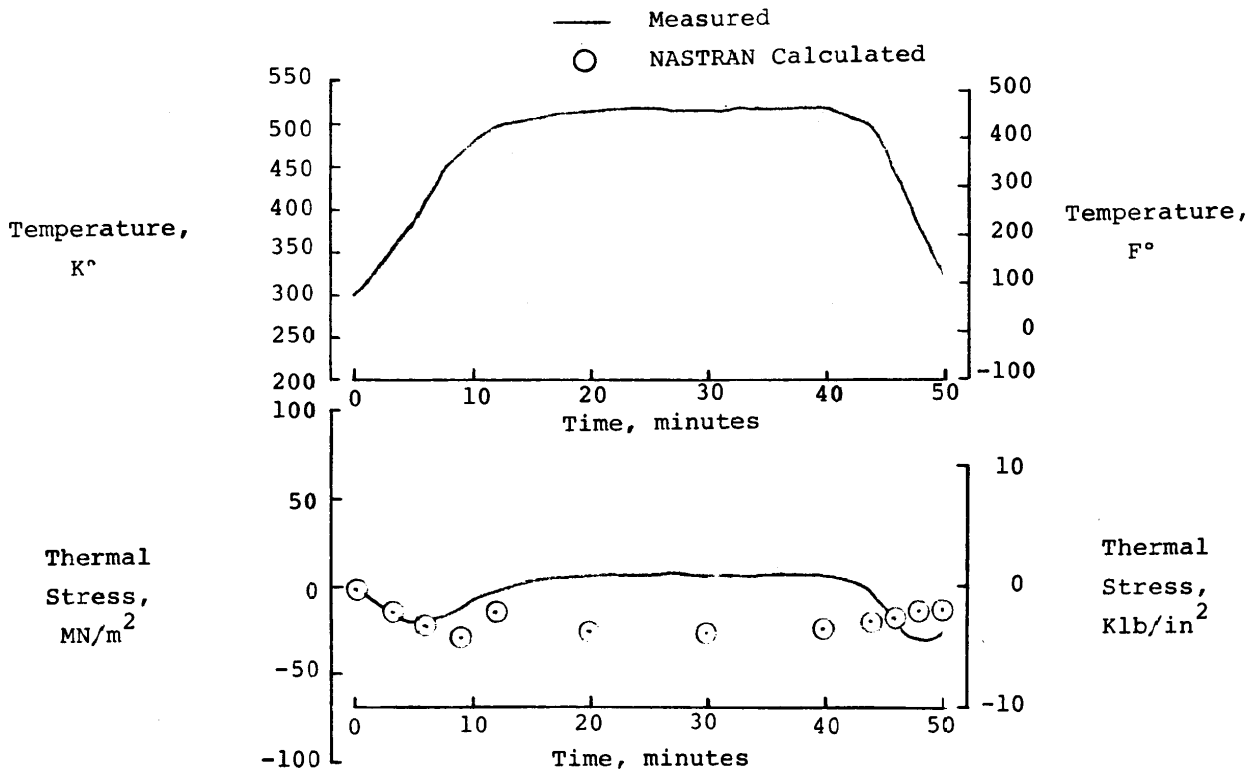

(p) Location M.

Figure 12. Concluded.

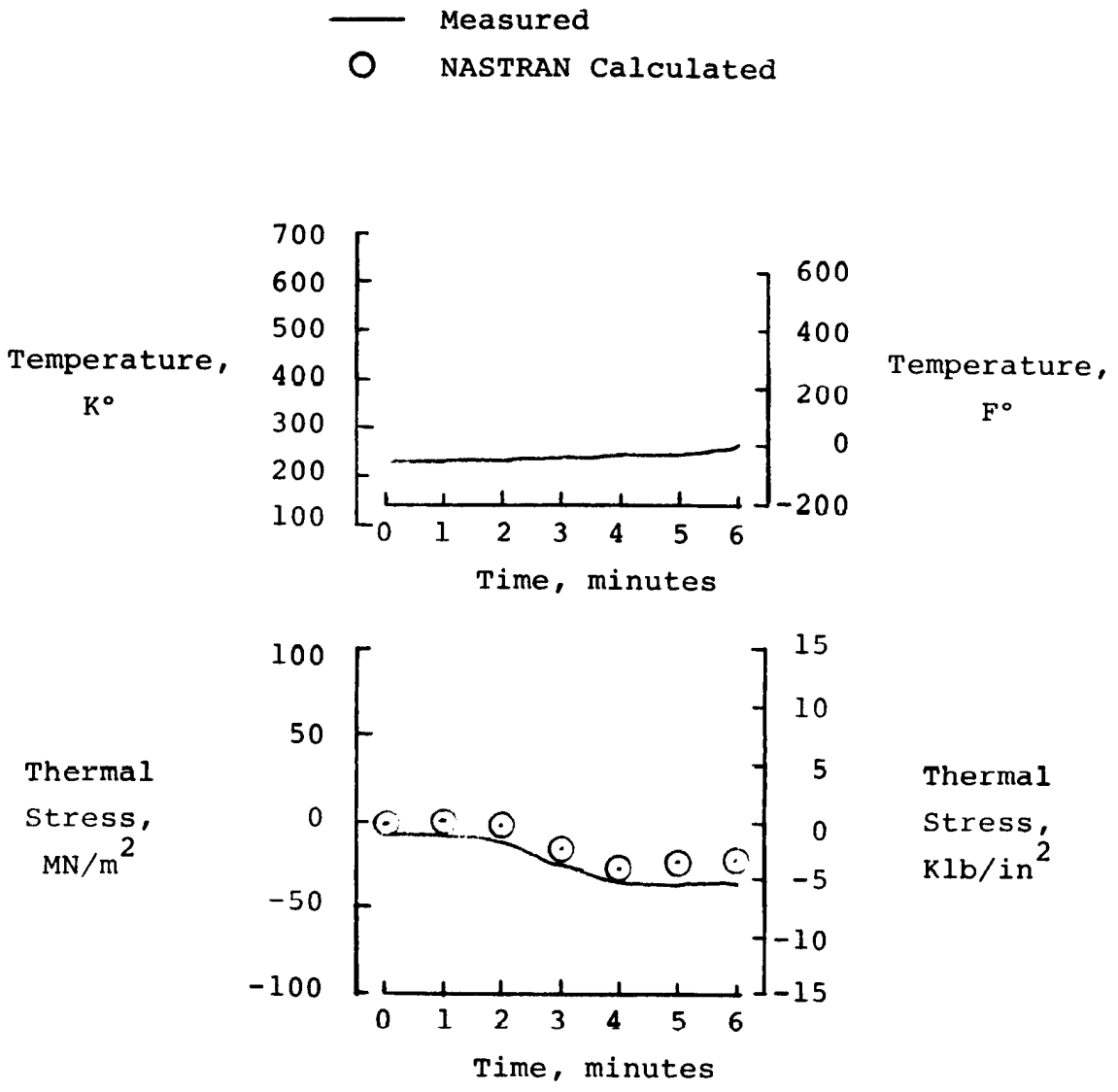

(a) Location A.

Figure 13. Measured temperatures and comparison of measured and NASTRAN-calculated thermal stresses for hypersonic heating simulation.

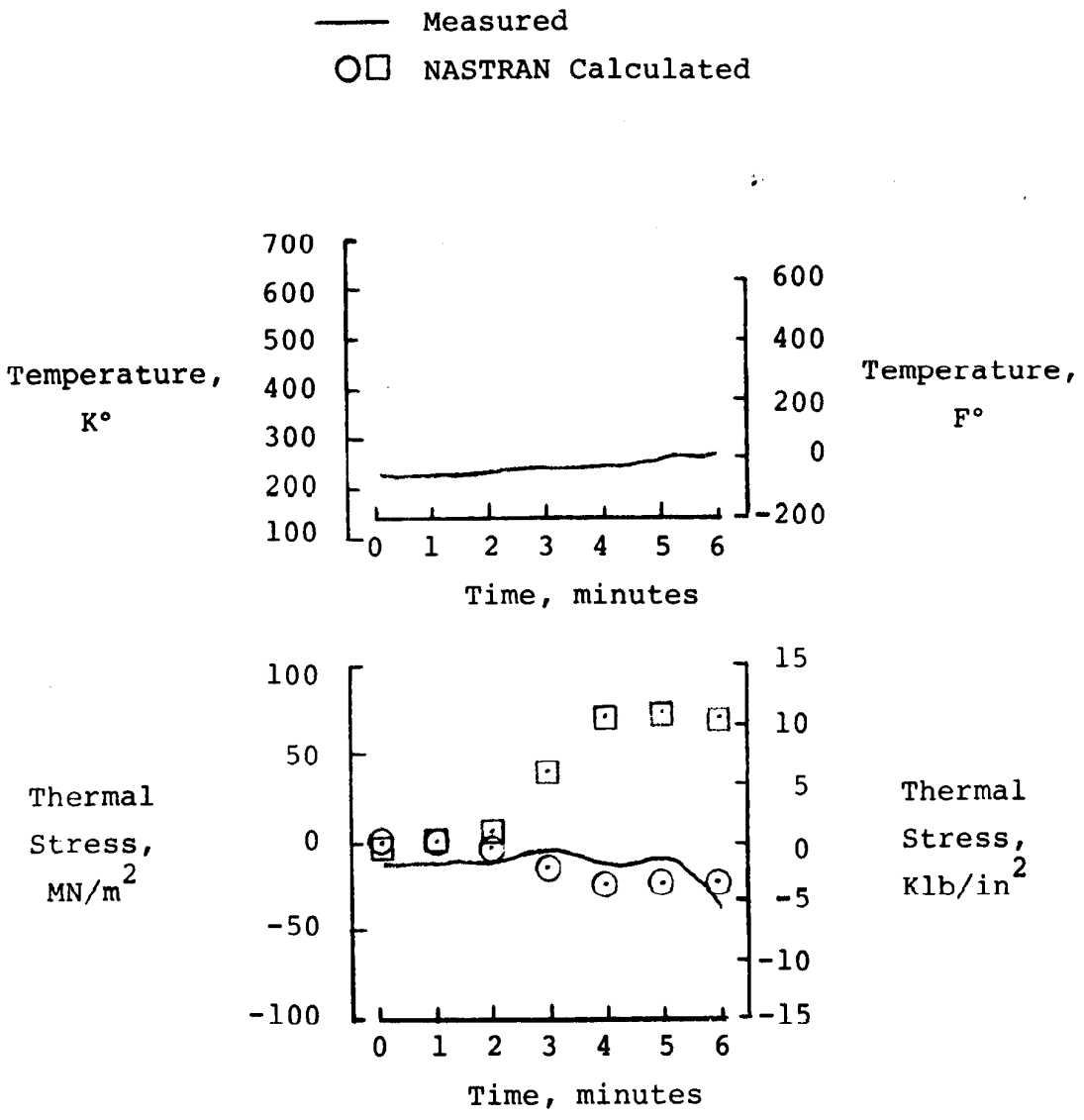

(b) Location B.

Figure 13. Continued.

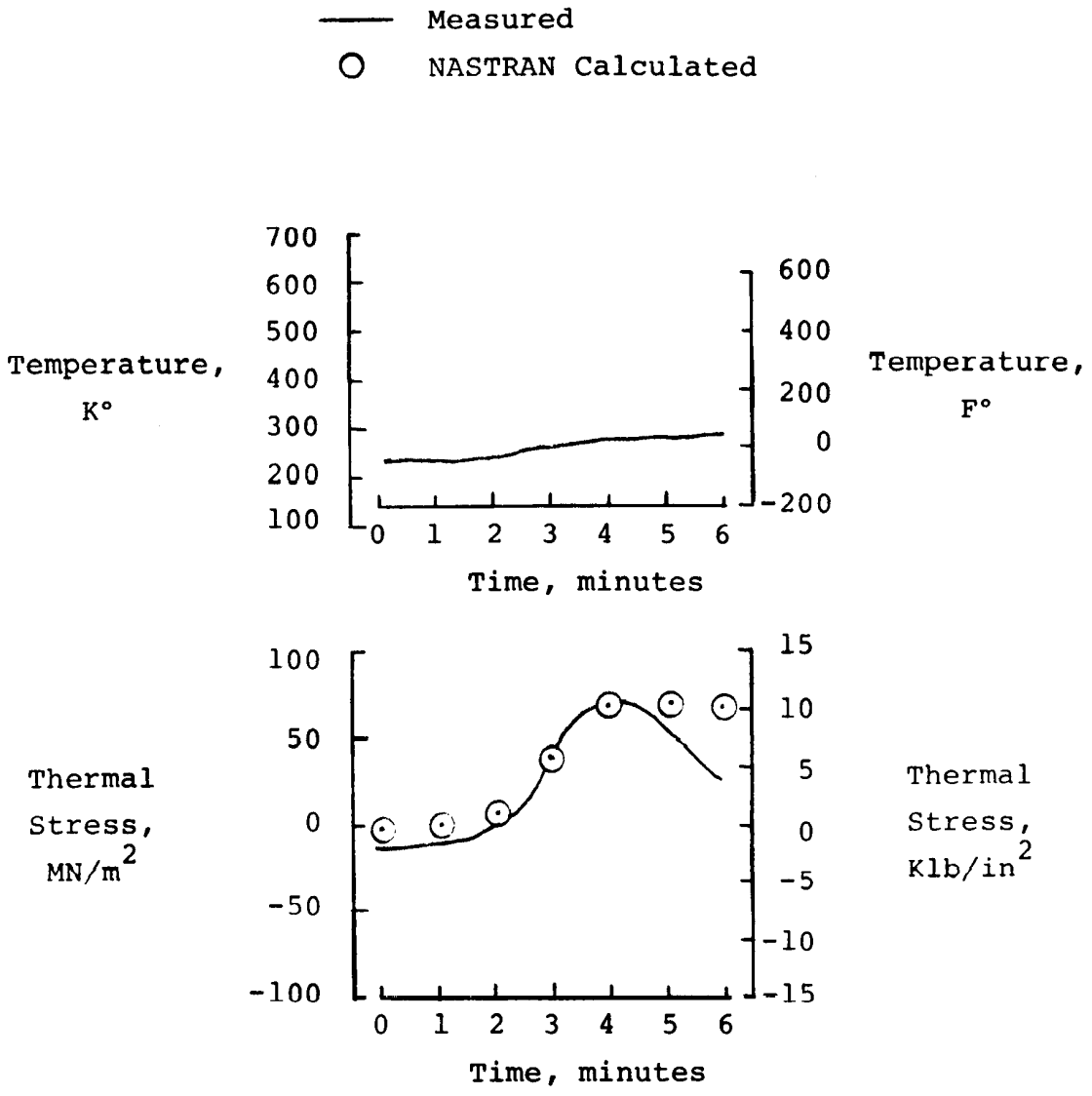

(c) Location C.

Figure 13. Continued.

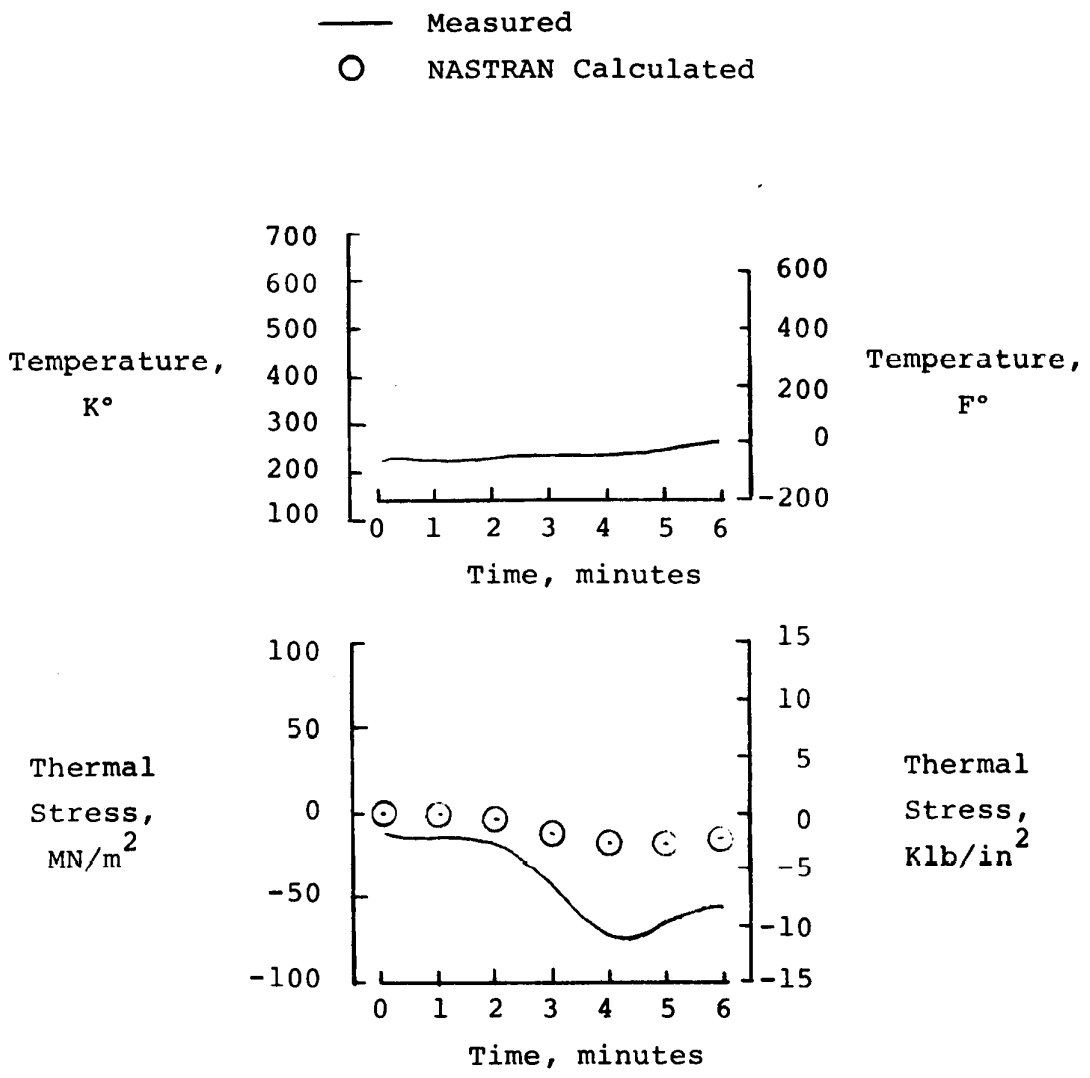

(d) Location R.

Figure 13. Continued.

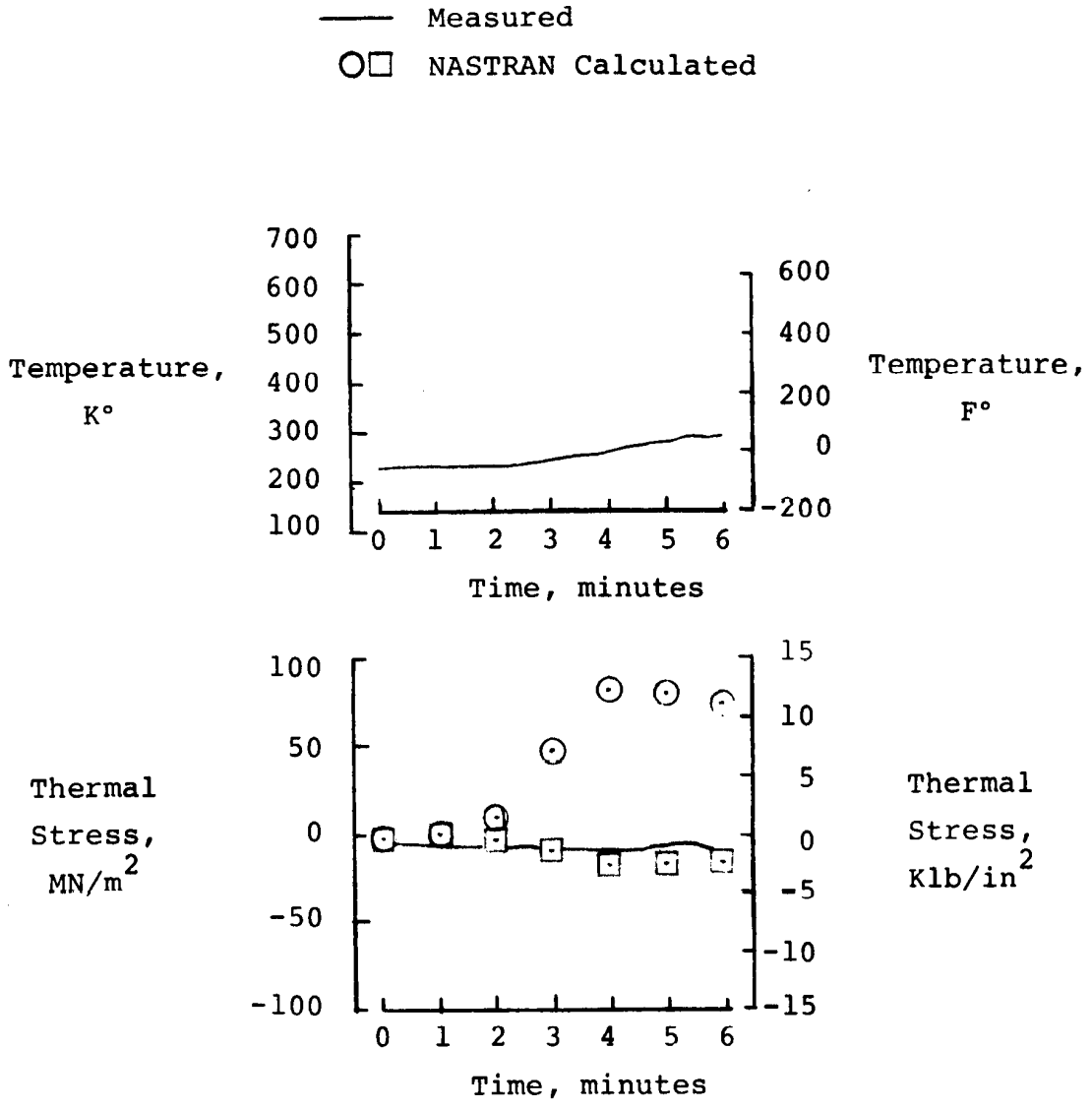

(e) Location Q.

Figure 13. Continued.

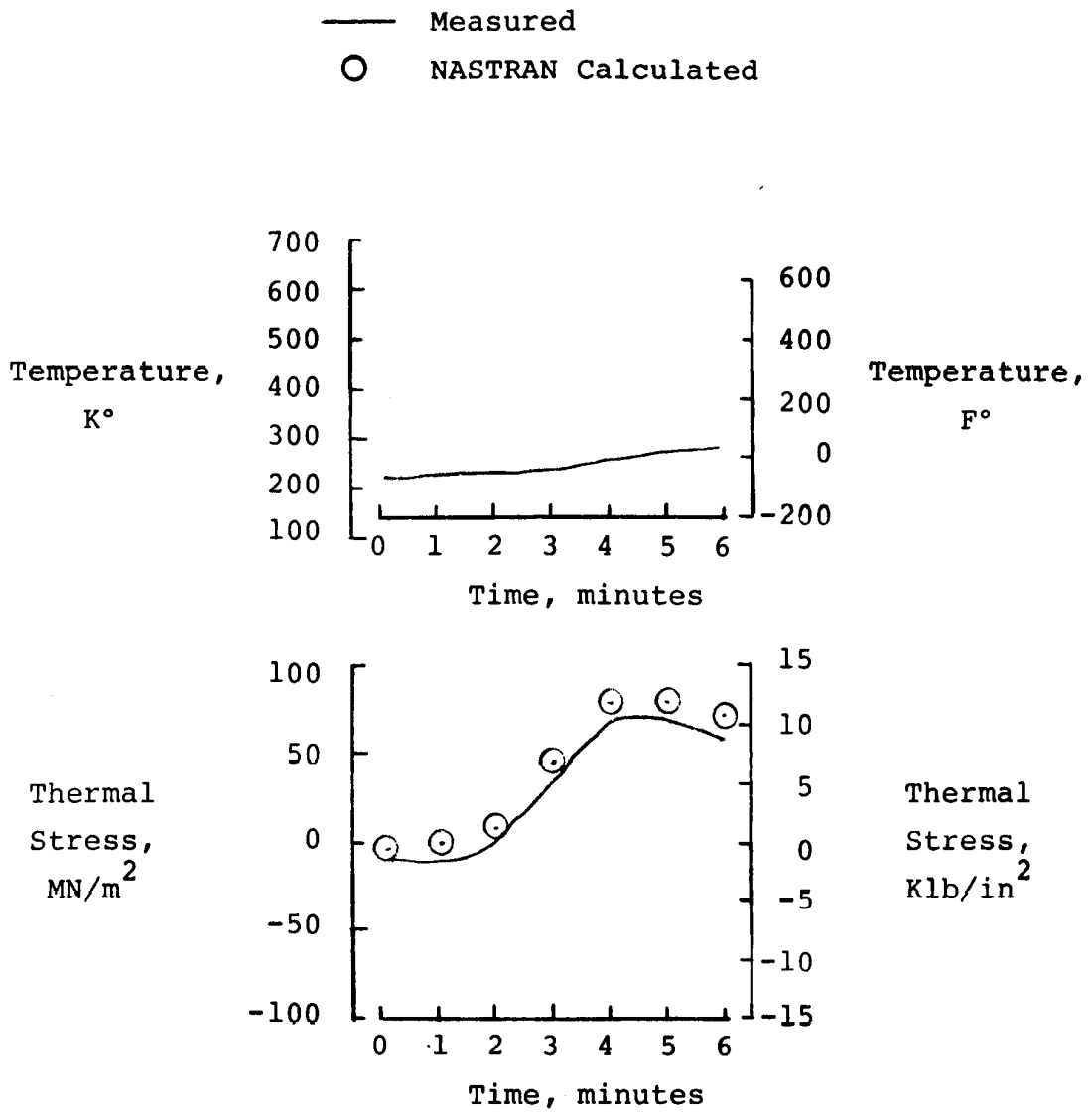

(f) Location P.

Figure 13. Continued.

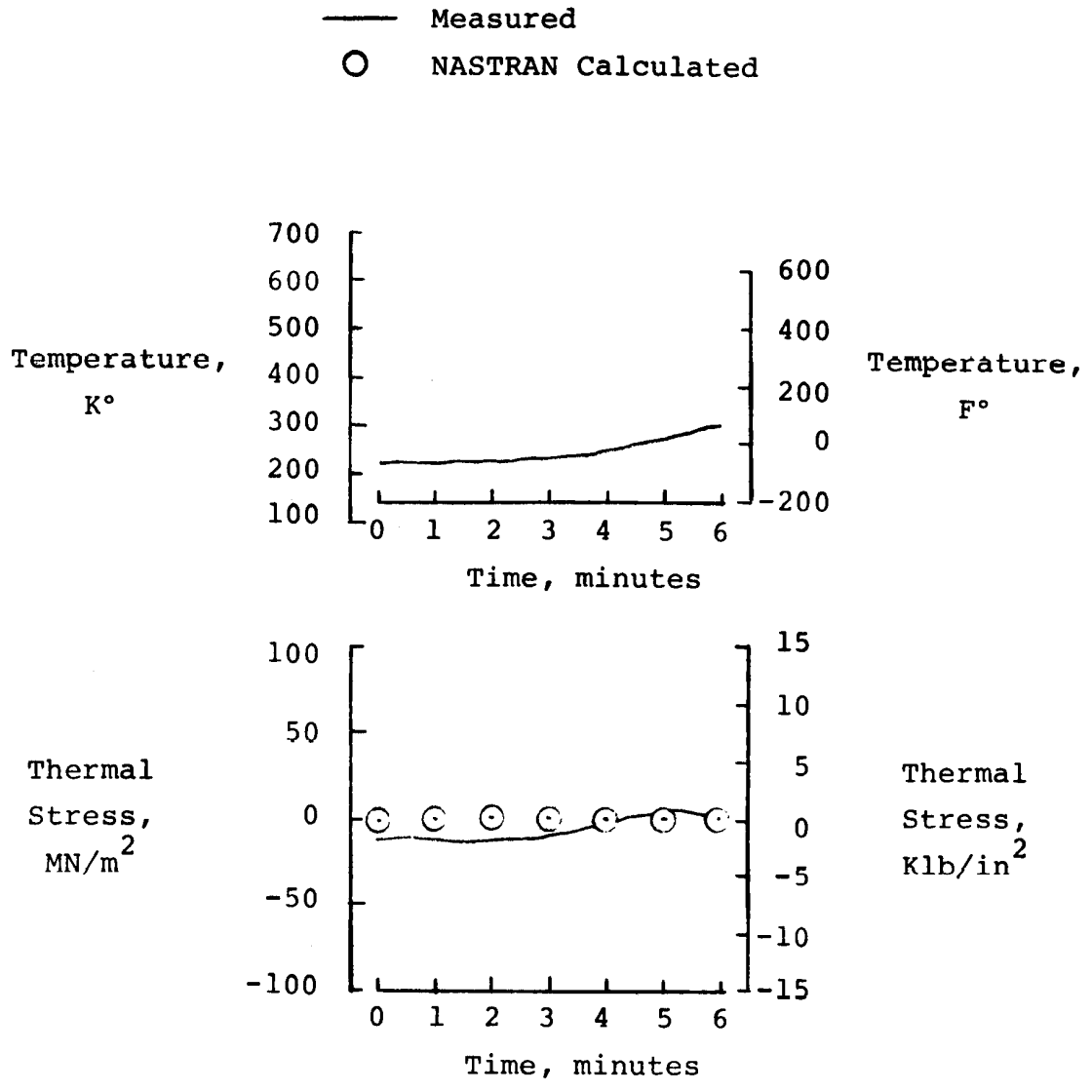

(g) Location O.

Figure 13. Continued.

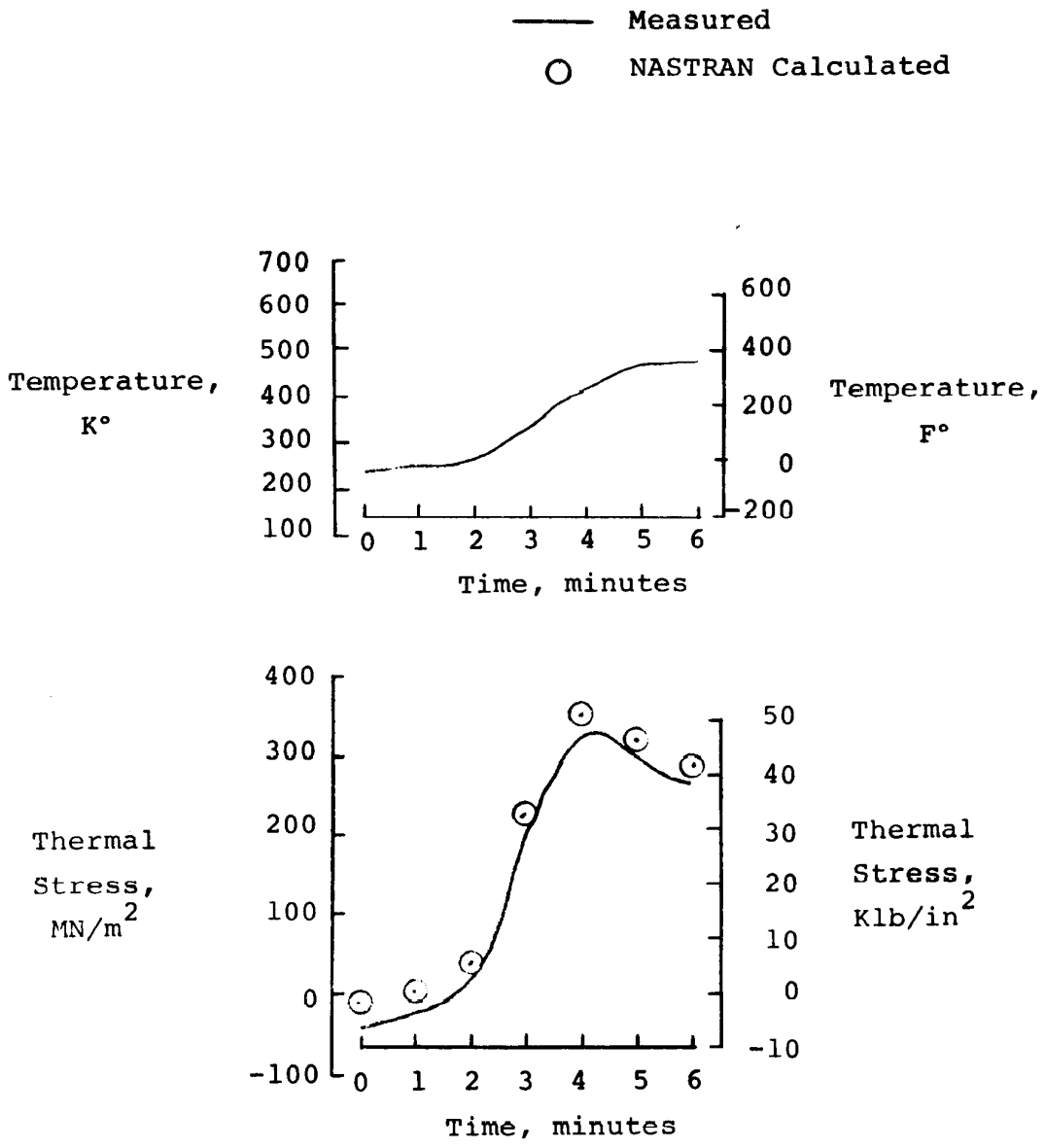

(h) Location E.

Figure 13. Continued.

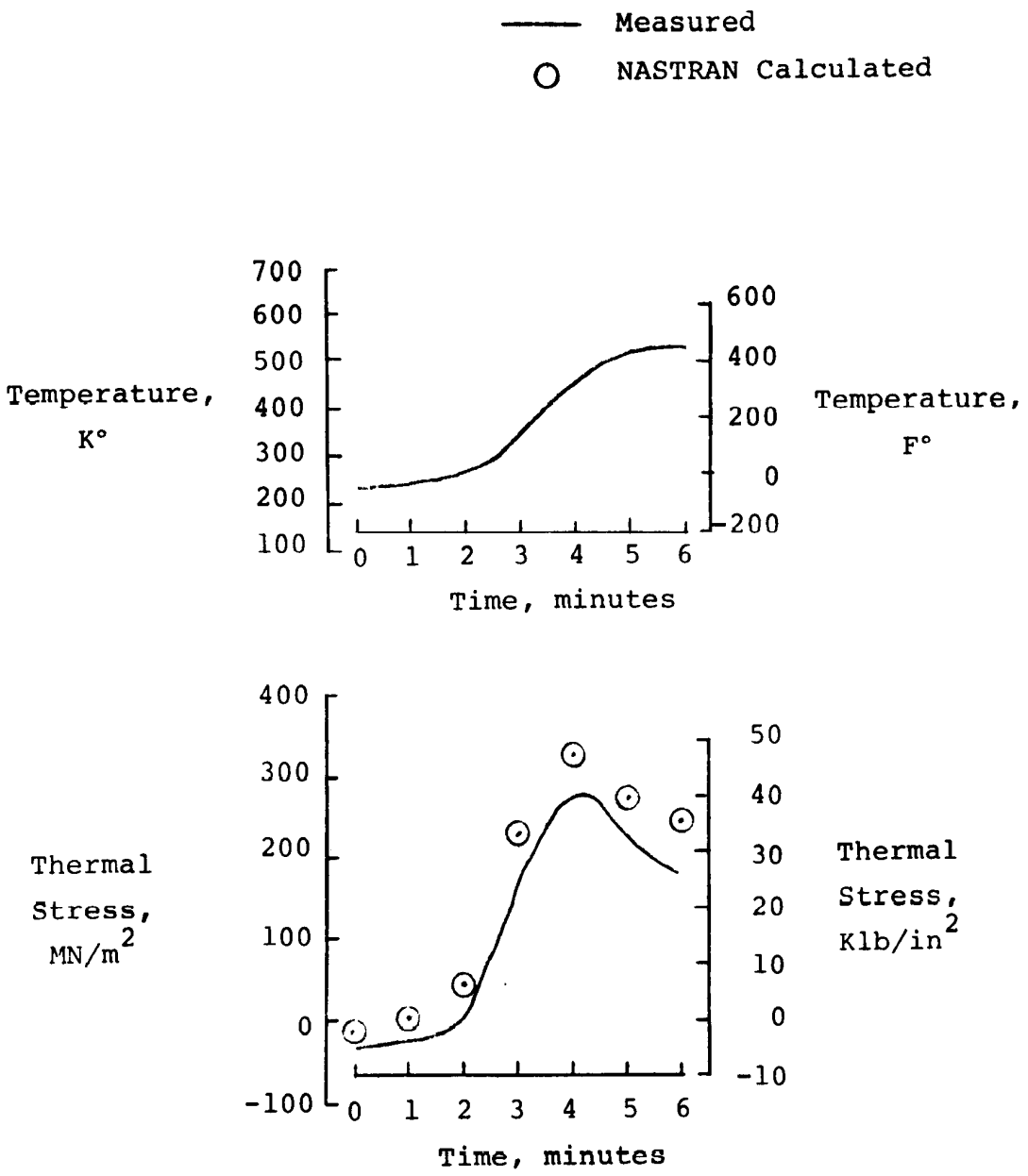

(i) Location N.

Figure 13. Continued.

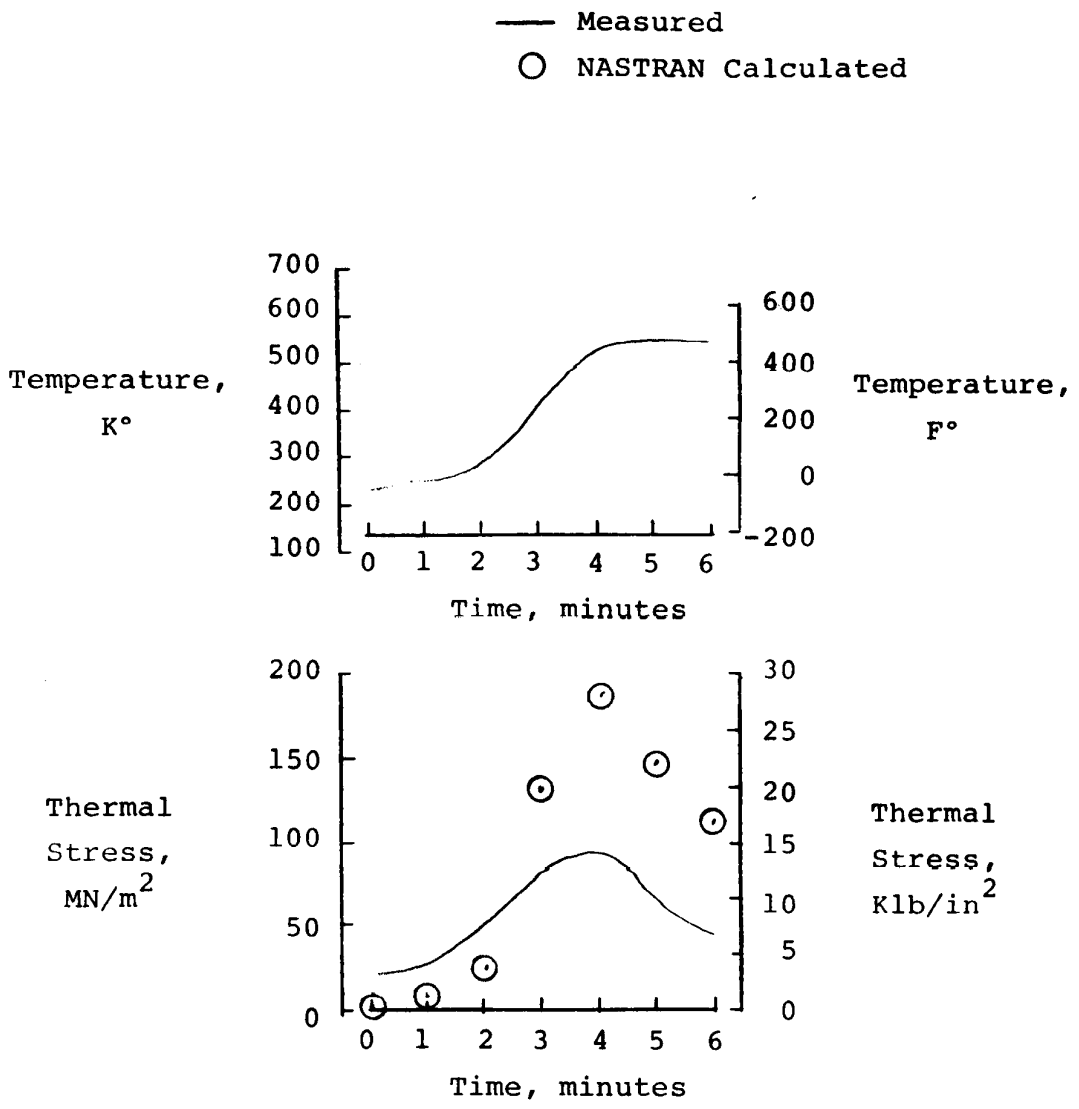

(j) Location F.

Figure 13. Continued.

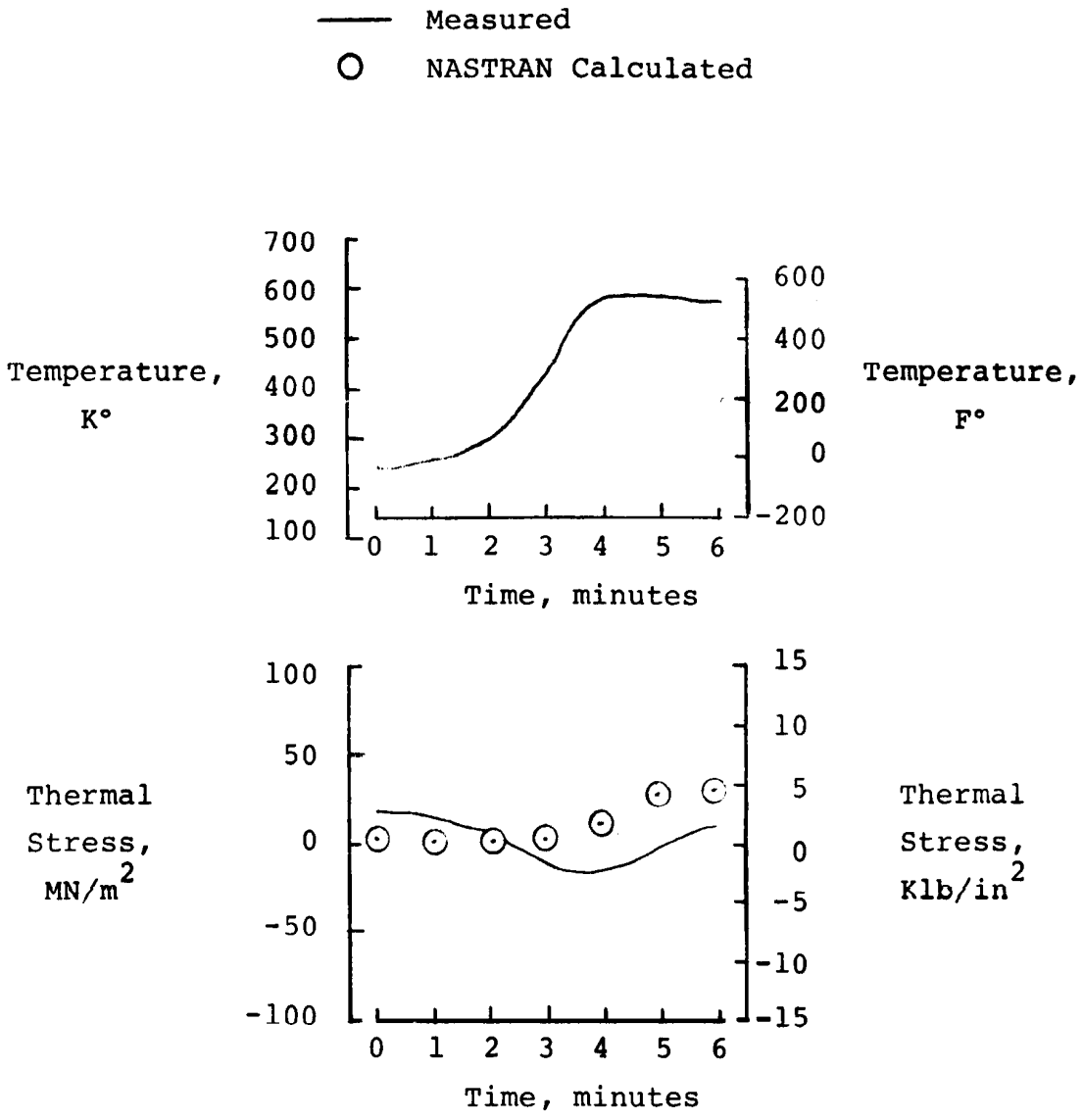

(k) Location G.

Figure 13. Continued.

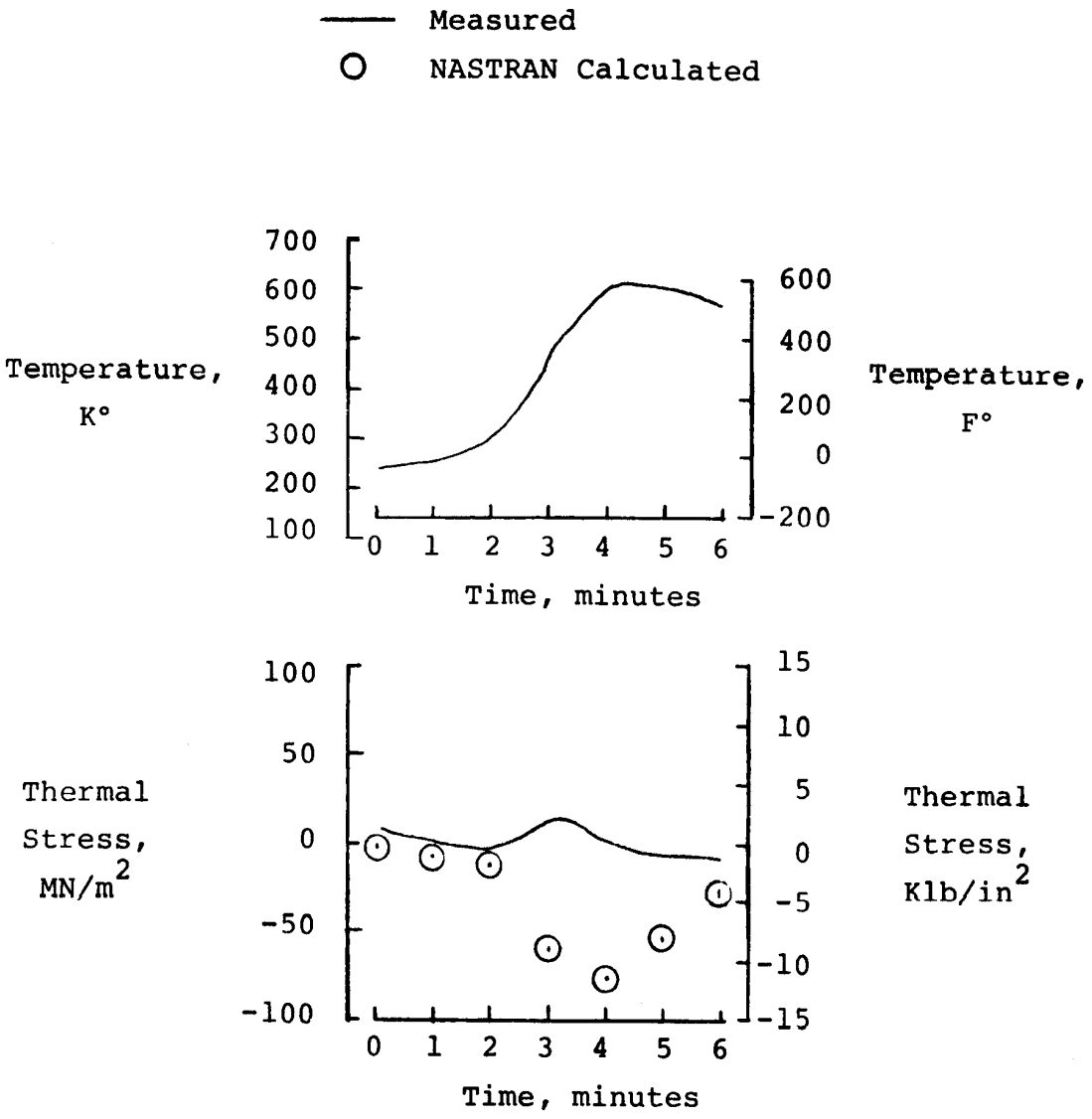

(l) Location H.

Figure 13. Continued.

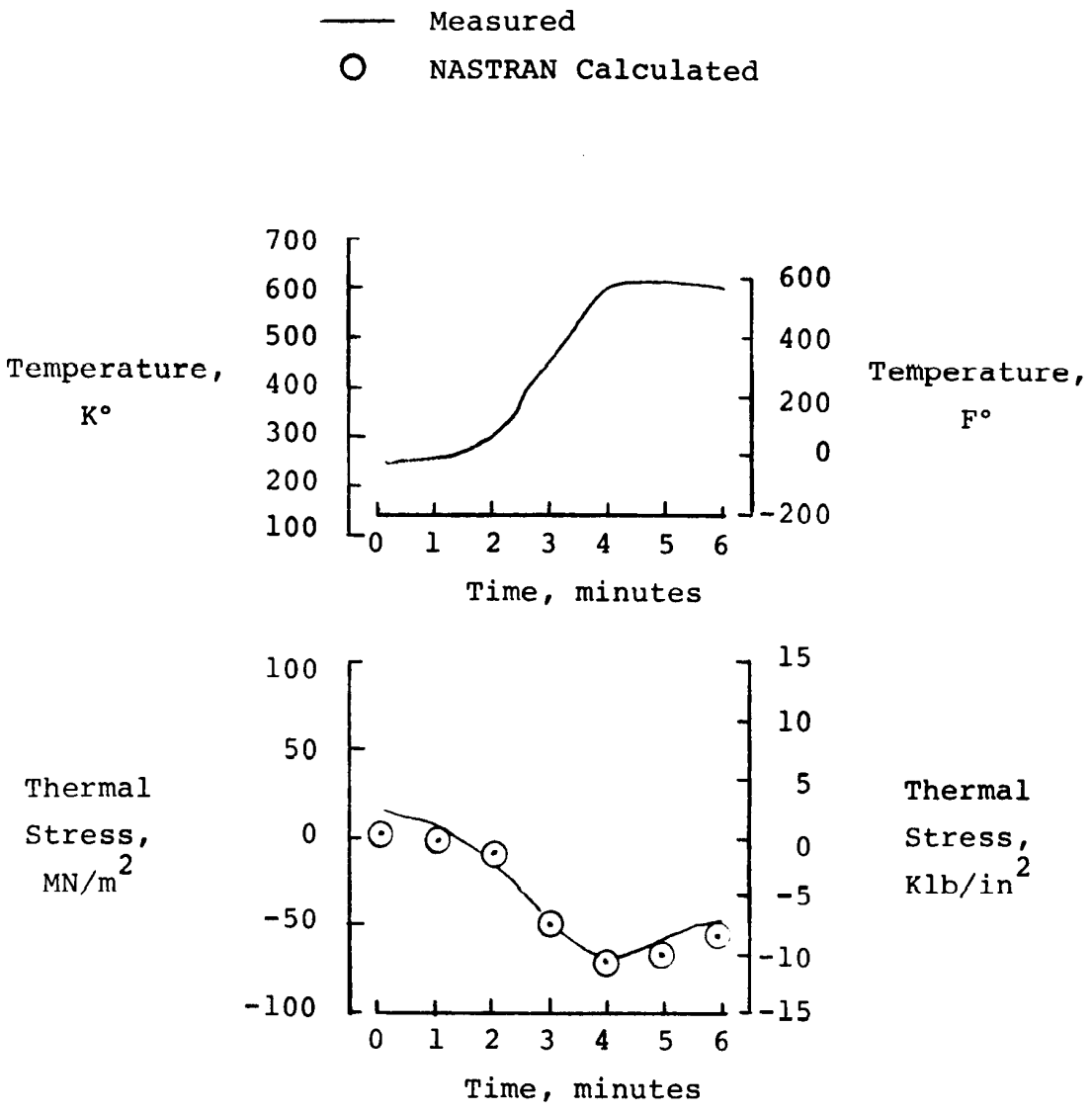

(m) Location I.

Figure 13. Continued.

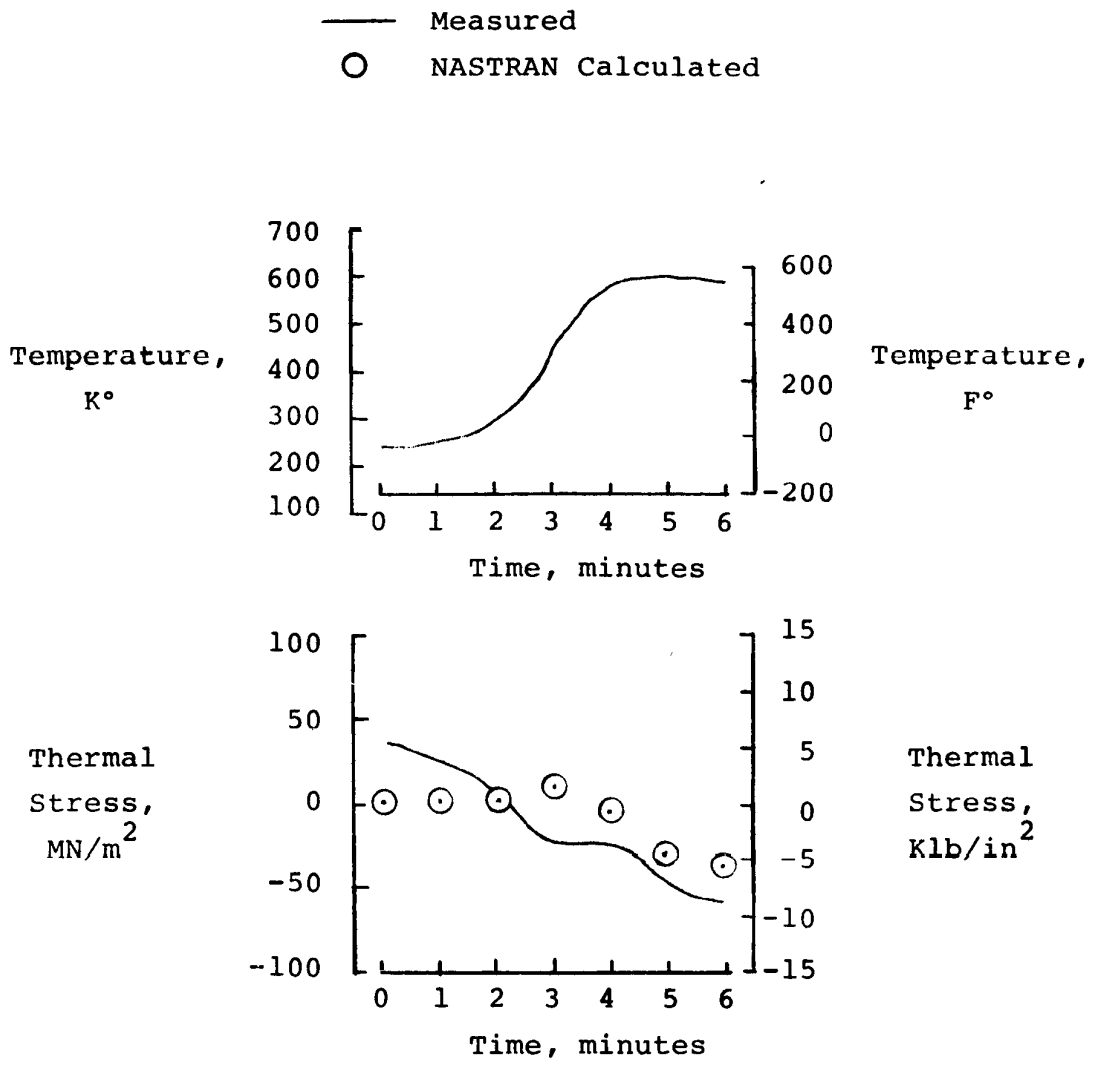

(n) Location J.

Figure 13. Continued.

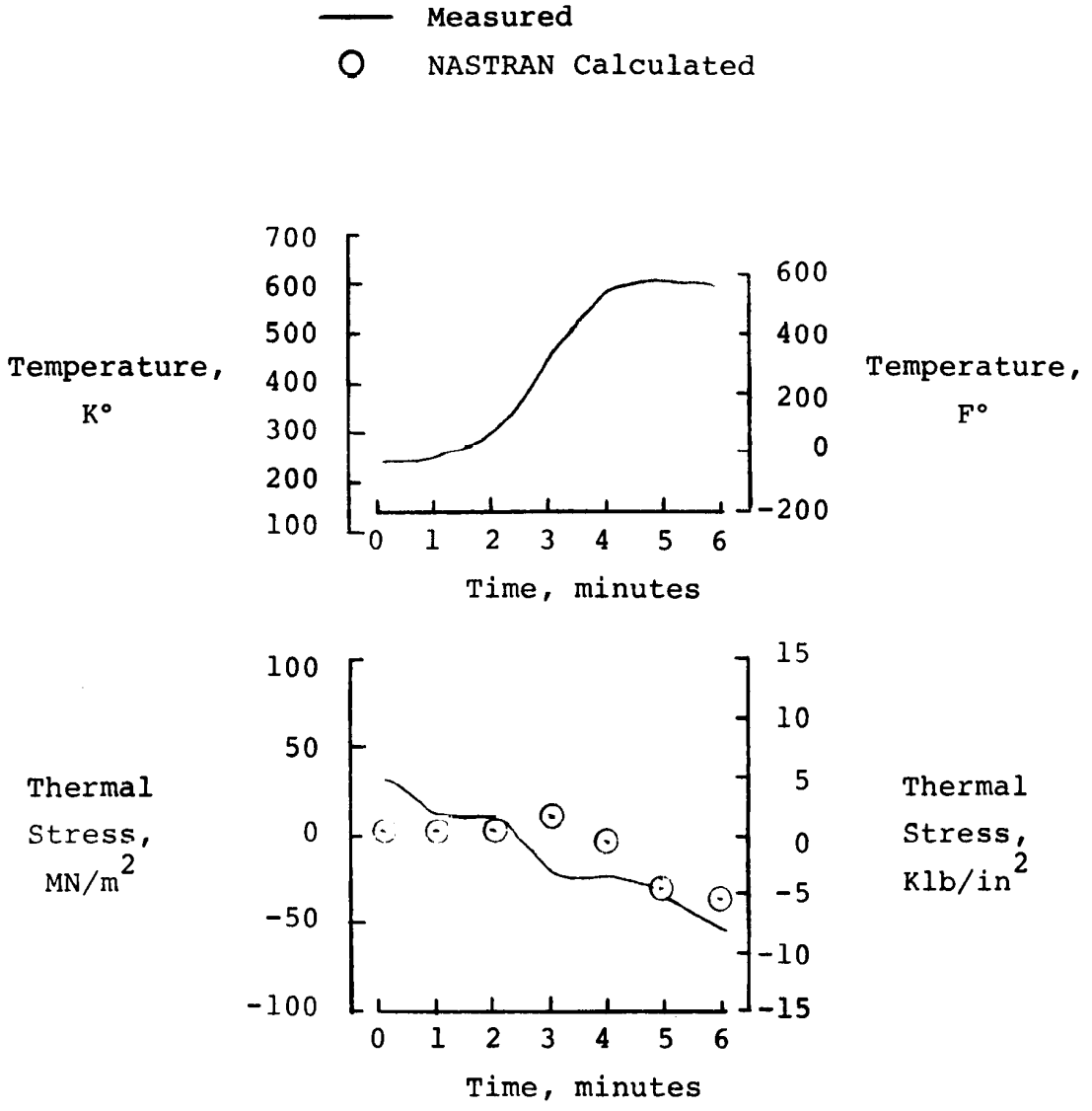

(o) Location K.

Figure 13. Continued.

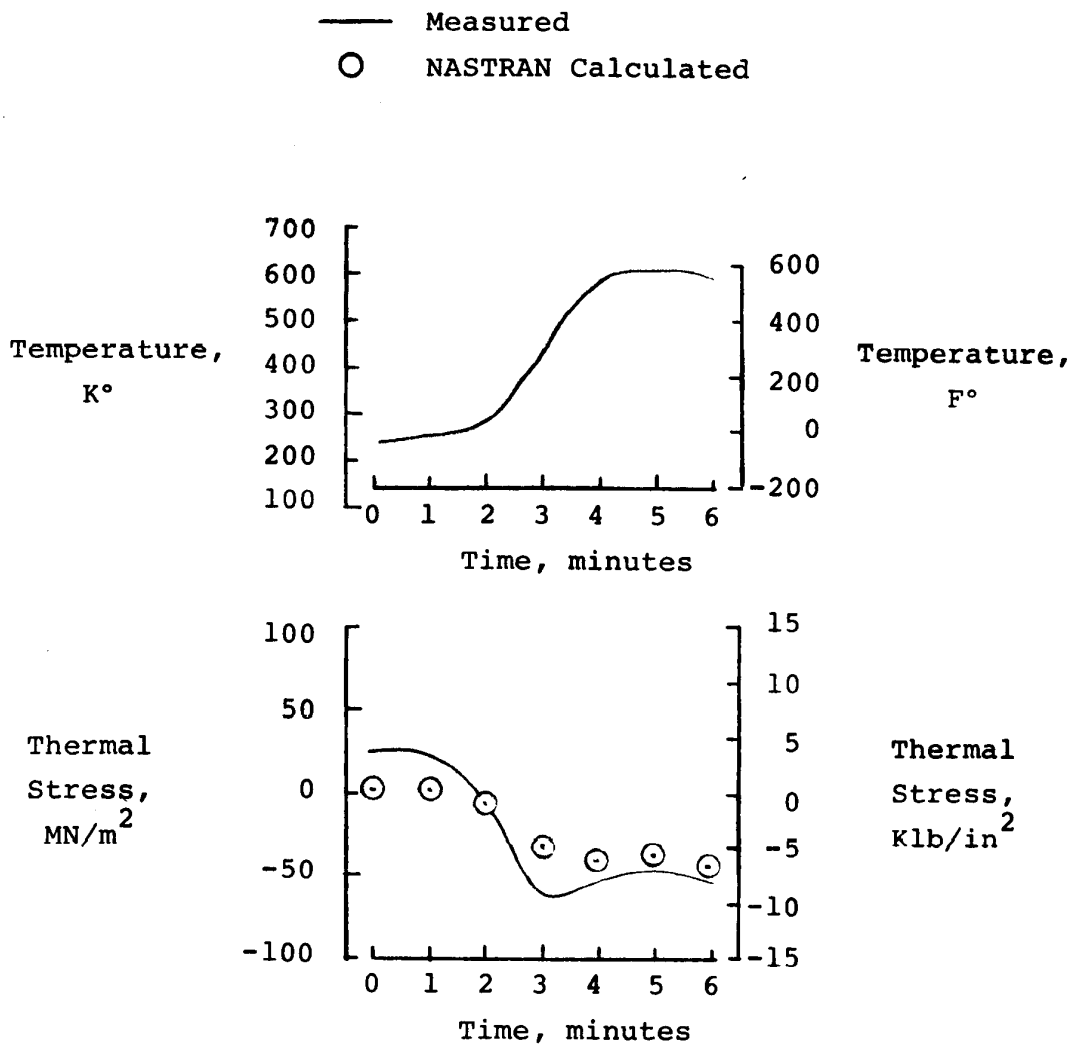

(p) Location L.

Figure 13. Continued.

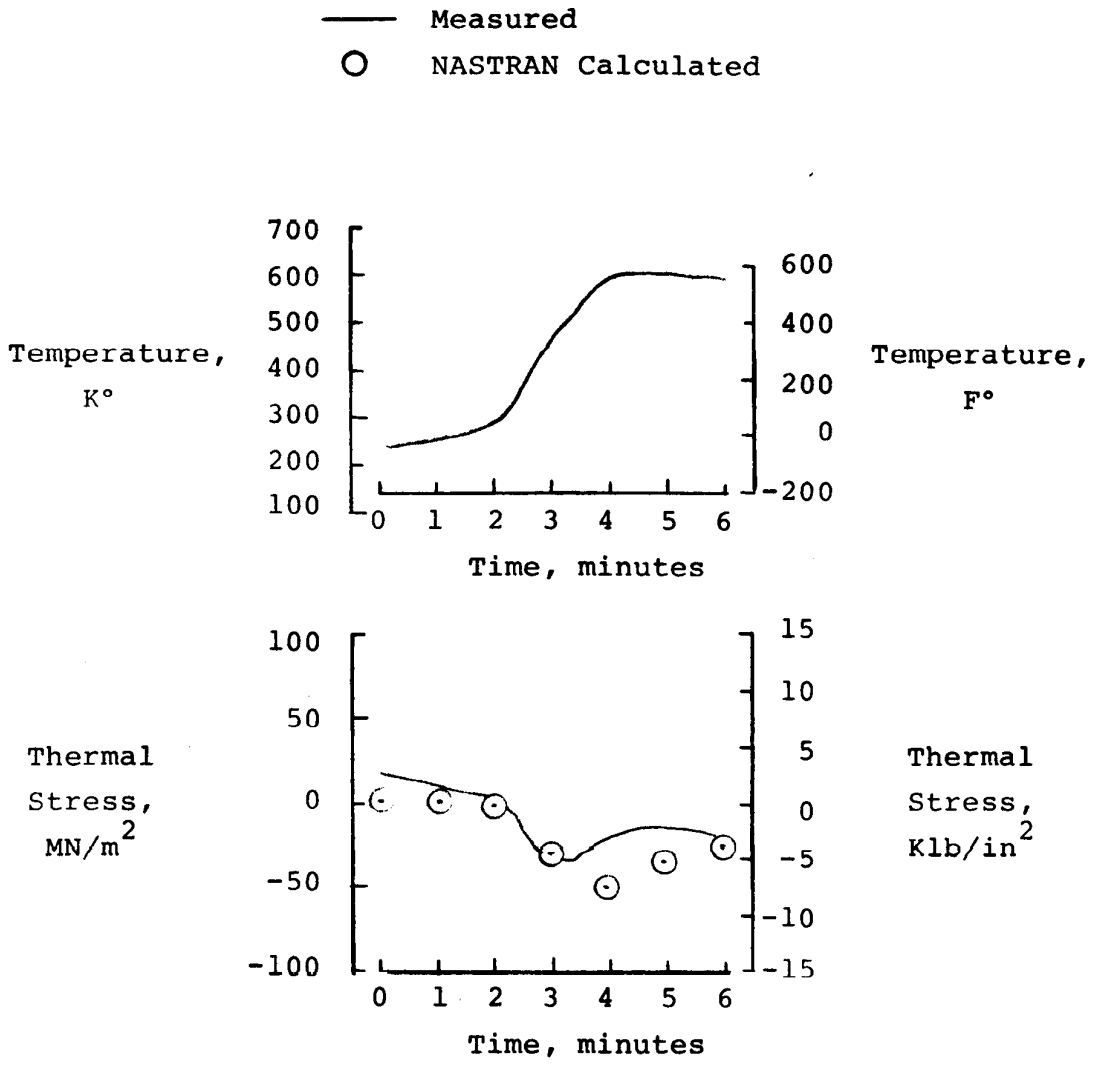

(q) Location M.

Figure 13. Concluded.

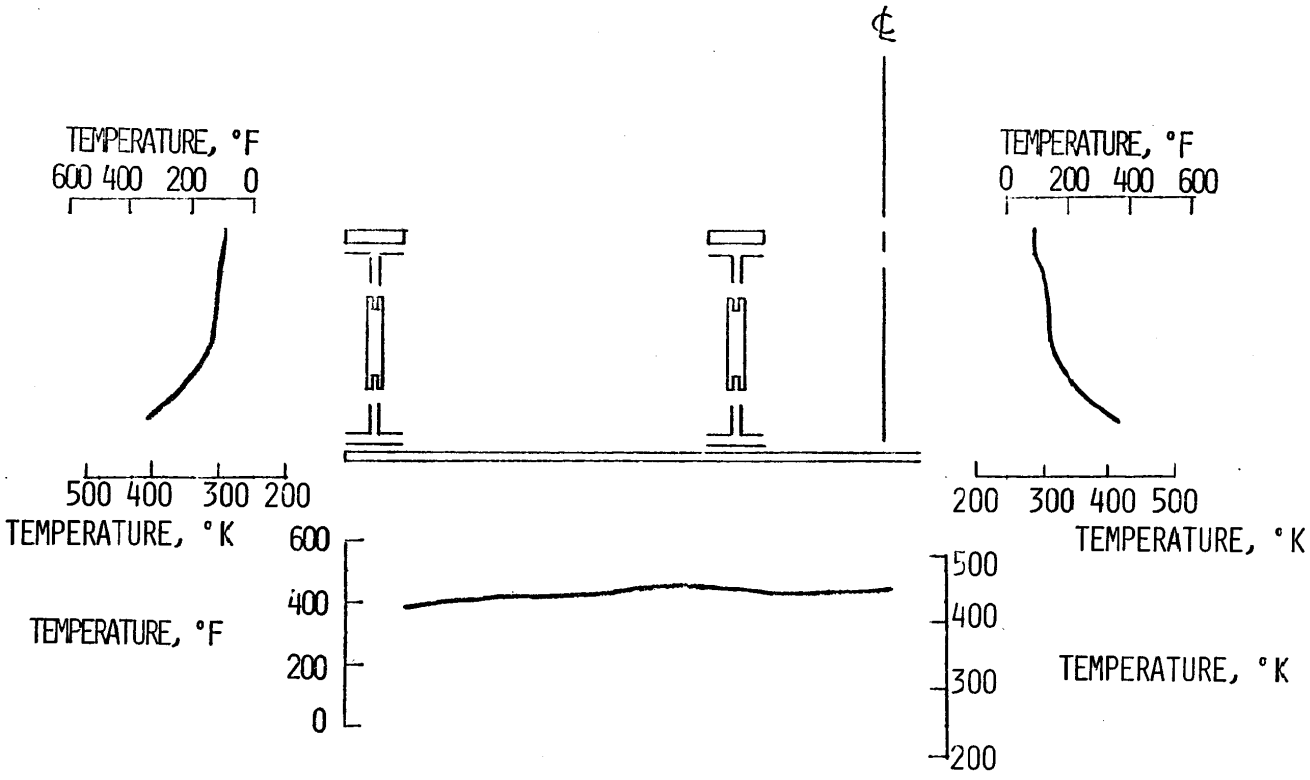

Figure 14. Distribution of measured temperatures for the supersonic case. Time = 12 minutes.

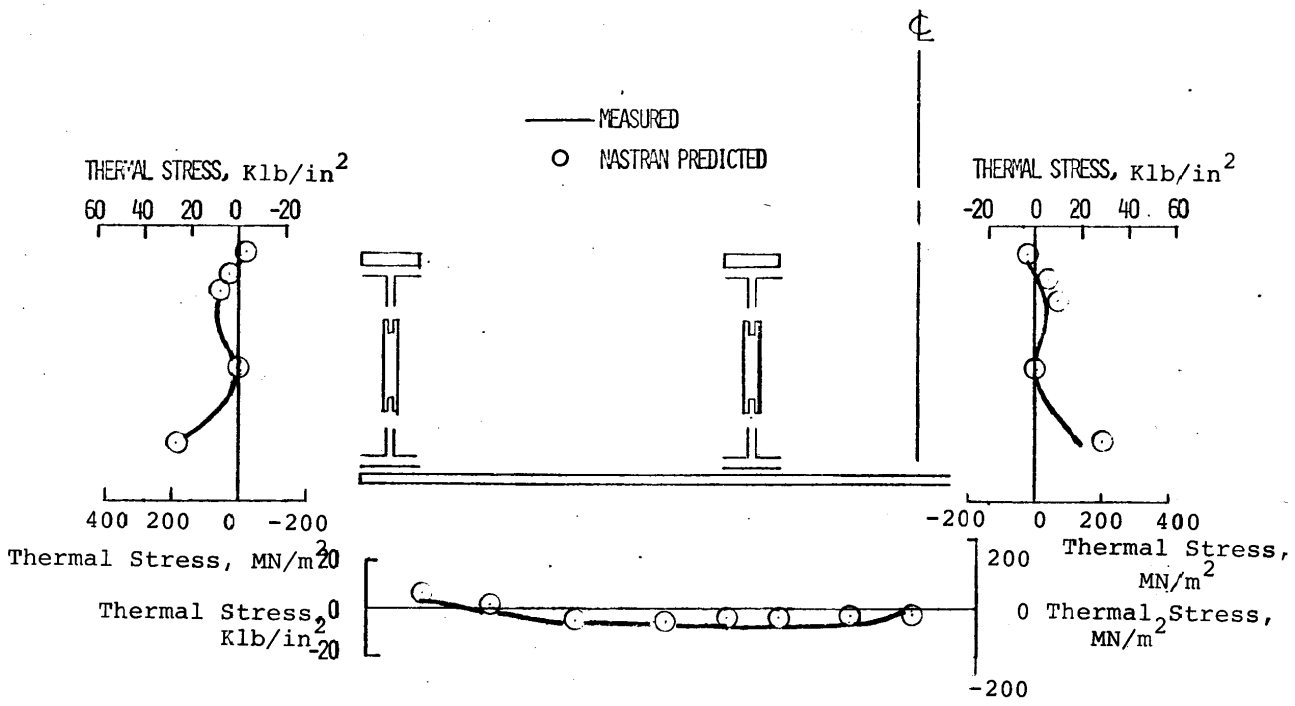

Figure 15. Comparison of measured and NASTRAN-calculated thermal stress distribution for the supersonic case. Time = 12 minutes.

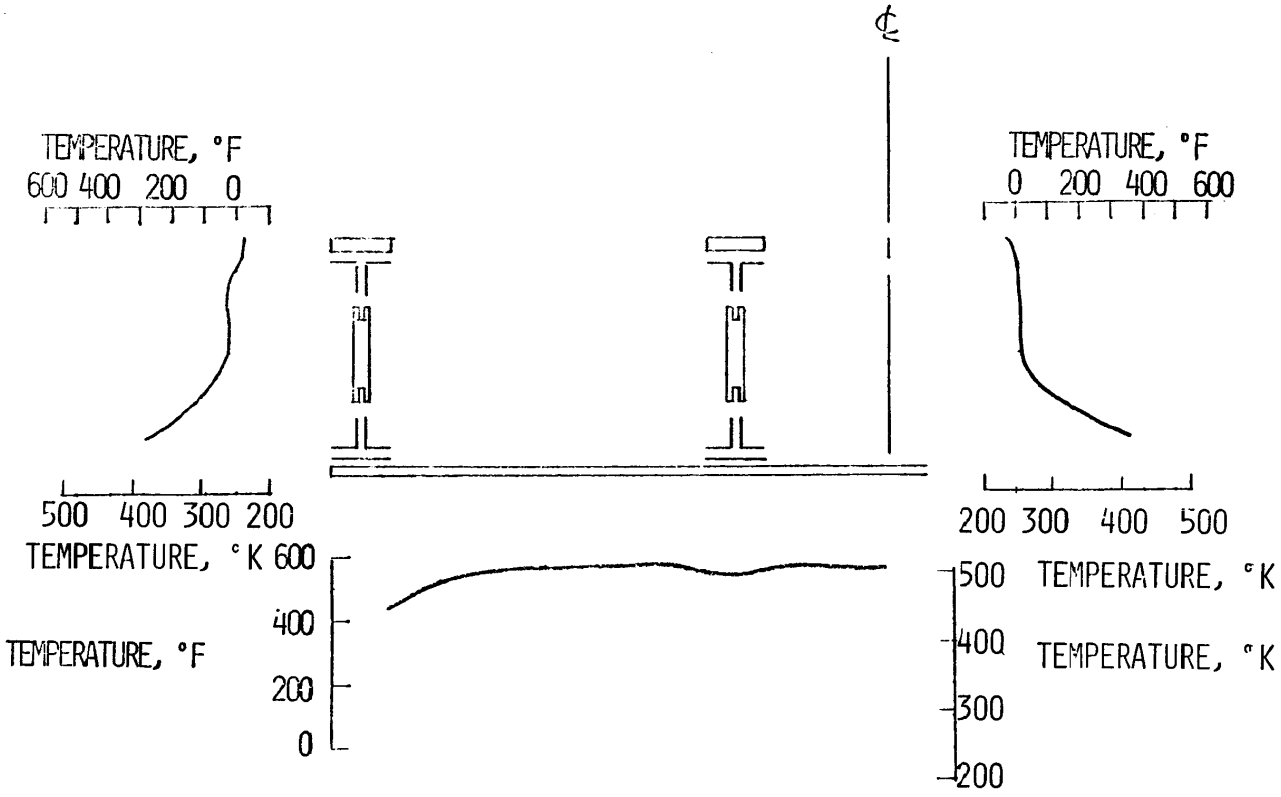

Figure 16. Distribution of measured temperatures for the hypersonic case. Time = 4 minutes.

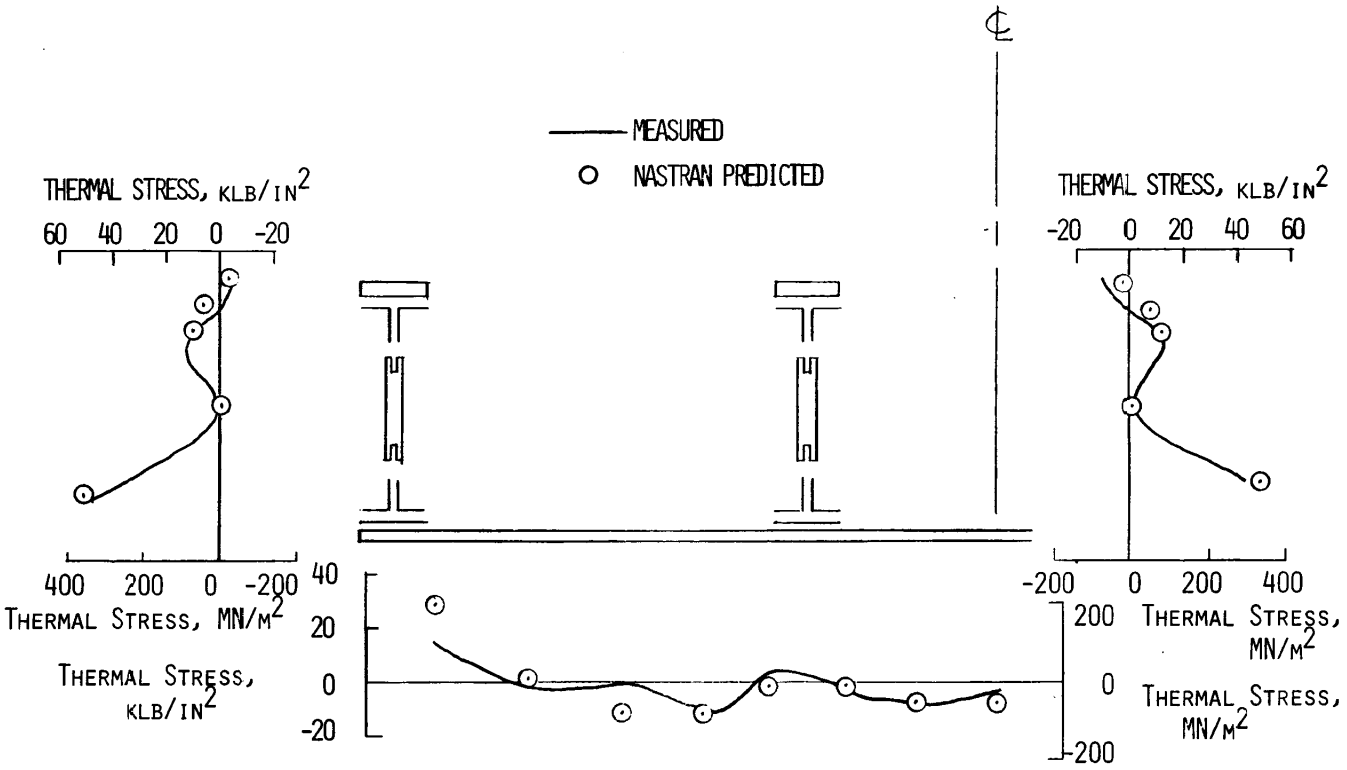

Figure 17. Comparison of measured and NASTRAN-calculated thermal stress distribution for the hypersonic case. Time = 4 minutes.

1. Report No. NASA TM-72857	2. Government Accession No.	3. Recipient's Catalog No.
4. Title and Subtitle CORRELATION OF PREDICTED AND MEASURED THERMAL STRESSES ON A TRUSS-TYPE AIRCRAFT STRUCTURE		5. Report Date November 1978 6. Performing Organization Code
7. Author(s) Jerald M. Jenkins, Lawrence S. Schuster, and Alan L. Carter		8. Performing Organization Report No. H-1074
9. Performing Organization Name and Address NASA Dryden Flight Research Center P.O. Box 273 Edwards, California 93523		10. Work Unit No. 505-02-24 11. Contract or Grant No.
12. Sponsoring Agency Name and Address National Aeronautics and Space Administration Washington, D.C. 20546		13. Type of Report and Period Covered Technical Memorandum 14. Sponsoring Agency Code
15. Supplementary Notes		

16. Abstract

A test structure representing a portion of a hypersonic vehicle was instrumented with strain gages and thermocouples. This test structure was then subjected to laboratory heating representative of supersonic and hypersonic flight conditions. A finite element computer model of this structure was developed using several types of elements with the NASA structural analysis (NASTRAN) computer program. Temperature inputs from the test were used to generate predicted model thermal stresses and these were correlated with the test measurements.

17. Key Words (Suggested by Author(s))	18. Distribution Statement
Thermal stresses Hypersonic structures	Unclassified—Unlimited STAR category: 01

19. Security Classif. (of this report)	20. Security Classif. (of this page)	21. No. of Pages	22. Price*
Unclassified	Unclassified	57	$4.25

For sale by the National Technical Information Service, Springfield, Virginia 22161